



Government of **Western Australia**
Department of **Mines, Industry Regulation and Safety**

RECORD 2018/5

A PETROGRAPHIC AND GEOCHRONOLOGICAL ASSESSMENT OF THE GABBROIC AND METAGABBROIC ROCKS OF THE FRASER ZONE, ALBANY–FRASER OROGEN, WESTERN AUSTRALIA

by
K Glasson



Geological Survey of Western Australia



Curtin University



Government of **Western Australia**
Department of **Mines, Industry Regulation and Safety**

Record 2018/5

A PETROGRAPHIC AND GEOCHRONOLOGICAL ASSESSMENT OF THE GABBROIC AND METAGABBROIC ROCKS OF THE FRASER ZONE, ALBANY–FRASER OROGEN, WESTERN AUSTRALIA

by
K Glasson

Perth 2018



**Geological Survey of
Western Australia**

MINISTER FOR MINES AND PETROLEUM
Hon Bill Johnston MLA

DIRECTOR GENERAL, DEPARTMENT OF MINES, INDUSTRY REGULATION AND SAFETY
David Smith

EXECUTIVE DIRECTOR, GEOSCIENCE AND RESOURCE STRATEGY
Jeff Haworth

REFERENCE

The recommended reference for this publication is:

Glasson, K 2018, A petrographic and geochronological assessment of the gabbroic and metagabbroic rocks of the Fraser Zone, Albany–Fraser Orogen, Western Australia: Geological Survey of Western Australia, Record 2018/5, 57p.

ISBN PDF 978-1-74168-800-9; Print 978-1-74168-801-6

Grid references in this publication refer to the Geocentric Datum of Australia 1994 (GDA94). Locations mentioned in the text are referenced using Map Grid Australia (MGA) coordinates, Zone 51. All locations are quoted to at least the nearest 100 m.

About this publication

This Record is an Honours thesis researched, written and compiled as part of a collaborative project between the Geological Survey of Western Australia (GSWA) and Curtin University, Perth. Although GSWA has provided support for this project, the scientific content of the Record, and the drafting of figures, was the responsibility of the author. No editing has been undertaken by GSWA.



Disclaimer

This product was produced using information from various sources. The Department of Mines, Industry Regulation and Safety (DMIRS) and the State cannot guarantee the accuracy, currency or completeness of the information. Neither the department nor the State of Western Australia nor any employee or agent of the department shall be responsible or liable for any loss, damage or injury arising from the use of or reliance on any information, data or advice (including incomplete, out of date, incorrect, inaccurate or misleading information, data or advice) expressed or implied in, or coming from, this publication or incorporated into it by reference, by any person whosoever.

Published 2018 by the Geological Survey of Western Australia

This Record is published in digital format (PDF) and is available online at <www.dmp.wa.gov.au/GSWApublications>.



© State of Western Australia (Department of Mines, Industry Regulation and Safety) 2018

With the exception of the Western Australian Coat of Arms and other logos, and where otherwise noted, these data are provided under a Creative Commons Attribution 4.0 International Licence. (<http://creativecommons.org/licenses/by/4.0/legalcode>)

Further details of geological products and maps produced by the Geological Survey of Western Australia are available from:

Information Centre
Department of Mines, Industry Regulation and Safety
100 Plain Street
EAST PERTH WESTERN AUSTRALIA 6004
Telephone: +61 8 9222 3459 Facsimile: +61 8 9222 3444
www.dmp.wa.gov.au/GSWApublications

Cover image: Elongate salt lake on the Yilgarn Craton — part of the Moore–Monger paleovalley — here viewed from the top of Wownaminy Hill, 20 km southeast of Yalgoo, Murchison Goldfields. Photograph taken by I Zibra for the Geological Survey of Western Australia



Department of Applied Geology

Honours Manuscript 2017

A petrographic and geochronological assessment of the gabbroic
and metagabbroic rocks of the Fraser Zone, Albany–Fraser
Orogen, Western Australia

Kate Josephine Glasson

16506581

Curtin University, Bentley, Western Australia

Supervised by Dr Tim Johnson, Associate Professor Chris Kirkland, Dr Chris Clark and Dr Nicholas Gardiner

This research project is a requirement for the partial fulfilment of the unit 'ERTH4001 Geoscience Honours Dissertation' for degree 'MJRH-GEOLG v.1 Applied Geology Honours Major (BSc) (Honours)' at Curtin University

Affirmation of Research

The following is a break-down of the work conducted in the process of this study. This research primarily made use of thin sections provided by the Geological Survey of Western Australia from the Fraser Zone, in the Albany–Fraser Orogen, Western Australia. Thin sections of six samples were analysed using standard transmitted light microscopy with a Leica DC 2000 digital imaging system, a TESCAN Integrated Mineral Analyser (TIMA) and a MIRA3 Scanning Electron Microscope (SEM).

The TIMA instrument is funded by a grant from the Australian Research Council (LE140100150) and is operated by the John de Laeter Centre at Curtin University with the support of the Geological Survey of Western Australia, University of Western Australia and Murdoch University. Kelly Mergiot gave assistance in sample analyses using the TIMA.

The MIRA3 SEM used is located at Curtin University, analyses of zircons within samples was done with the assistance of Dr. Zakaria Quadir and PhD student Michael Hartnady.

The bulk major element compositions of six samples were measured by X-ray fluorescence (XRF). XRF chemical analyses were undertaken at Franklin and Marshall College, Pennsylvania. Phase equilibria modelling was conducted at Curtin University for all six samples with the help and supervision of Dr Tim Johnson and Ms Eleanore Blereau.

LA ICP-MS analyses and REE trace element geochemistry was conducted at Curtin University with the assistance of Prof. Noreen Evans, Bradley McDonald, Associate Professor Chris Kirkland. Initial processing of data was conducted using Iolite software package with the help of PhD students Julian Chard and Michael Hartnady.

Table of Contents

1.0 Introduction.....	6
2.0 Regional geology	6
2.1 Lithotectonic domains	6
2.2 Tectonomagmatic and metamorphic events	7
2.2.1 Biranup Orogeny.....	7
2.2.2 Albany Fraser Orogeny	8
2.3 Geology of the Fraser Zone	8
3.0 Methods and analytical techniques	10
3.1 Petrography	10
3.1.1 TESCAN Integrated Mineral Analyzer (TIMA)	10
3.2 XRF major element analysis and Fe-titration	10
3.3 Pseudosections	11
3.4 Geochronology and trace element geochemistry.....	11
4.1 Magmatic samples.....	12
4.1.1 Sample 216342	13
4.1.2 Sample 216355	13
4.1.3 Sample 216350	14
4.2 Metamorphic samples	14
4.2.1 Sample 183623	15
4.2.2 Sample 183661	15
4.2.3 Sample 183654	16
5.0 Mineral equilibria modelling	16
5.1 Magmatic Samples.....	16
5.2 Metamorphic Samples.....	17
6.0 U–Pb zircon geochronology	17
6.1 Sample 216342	18
6.2 Sample 183623	18
7.0 Discussion	18
7.1 Metamorphic evolution of the Fraser Zone	18
7.2 Age interpretation	19
7.3 Zircon	20
8.0 Conclusions.....	22
Acknowledgements	23
References	24
List of figures	27

List of tables.....29

List of appendices30

Figures31

Tables41

Appendices.....42

Abstract

Cratons represent the old, stable nuclei of continents, whose margins are subjected to intense reworking and which commonly host ancient mineral deposits. The Albany–Fraser Orogen (AFO) is an under-exposed and under-investigated region of a modified Archean craton margin. The Fraser Zone, one of the major lithotectonic domains of the AFO, lies in the north-eastern section of the Orogen. It is exposed over an area of some 425 x 50 km and is volumetrically dominated by gabbroic rocks and their metamorphosed equivalents. However, despite their abundance, little is known about their pressure–temperature–time (P–T–t) evolution. Phase equilibria modelling and U–Pb isotopic data from (meta) gabbroic rocks of the Fraser Zone constrain the overlapping crystallisation and/or peak condition to ~ 950 °C and ~ 7 kbar. U–Pb isotopic data constrain igneous crystallisation at c. 1295 ± 5 Ma and metamorphic zircon growth at c. 1293 ± 6 Ma. The occurrence of zircon growth due to magmatic crystallisation, in addition to a coronal zircon around ilmenite, suggests slow cooling of gabbros at high temperatures, facilitating diffusion of zirconium from ilmenite. This coronal texture combined with coeval ages of magmatic crystallisation and metamorphism elucidate the multiphase, prolonged nature of magmatism. These new data, combined with previous work, suggest that mafic magmatism was the thermal driver for granulite facies metamorphism in the Fraser Zone.

Keywords

Albany–Fraser Orogen, Fraser Zone, (meta) gabbroic, Pseudosection modelling, Zircon corona

1.0 Introduction

The curvilinear Albany–Fraser Orogen (AFO), on the southern and south-eastern margins of the Yilgarn Craton, provides valuable information in relation to the development of Proterozoic Australia and correlations between Australia and Antarctica (Morrissey et al., 2017). In addition, the recent discovery of the Nova Nickel sulphide deposit in the Fraser Zone (1305–1290 Ma), a major component of the AFO, has focussed economic attention on the region, in particular the mafic components (Fig.1) (Kirkland et al., 2016a).

Several studies have explored the metamorphic and structural history of the Fraser Range Metamorphics, where research has focussed primarily on metasedimentary rocks (e.g. (Spaggiari et al., 2011, Clark et al., 1999, Smithies et al., 2013, Clark et al., 2014). However, there are few geochronological studies constraining the absolute timing of emplacement and/or metamorphism of the volumetrically dominant (meta) gabbroic rocks of the Fraser Zone, and no detailed pressure–temperature (P – T) investigations of these rocks (De Waele and Pisarevsky, 2008, Clark et al., 1999). With the application of modern techniques, including phase equilibria modelling and *in situ* U–Pb isotopic dating, constraining the thermal evolution of the (meta) gabbros will permit a clearer understanding of the tectonic setting in which the rocks formed, with broader implications for mineralisation and the assembly and breakup of Rodinia.

2.0 Regional geology

The AFO, which extends for more than 1200km is divided into a number of fault bounded lithotectonic zones based on geophysical, geochemical and geochronological data. These subdivisions include the Archean Northern Foreland and the Kapa Kurl Booya Province (KKBP) (Spaggiari et al., 2009, Spaggiari et al., 2014, Occhipinti et al., 2017) (Fig. 2).

2.1 Lithotectonic domains

The Northern Foreland records the reworking of the Yilgarn Craton during the Albany–Fraser Orogeny. The southern portion of the Northern Foreland overlies the Yilgarn Craton as series of thrust sheets (Occhipinti et al., 2017, Spaggiari et al., 2009, Spaggiari et al., 2014), in which granitic rocks of the Munglinup Gneiss are surrounded by major faults (Spaggiari et al., 2011).

The Kapa Kurl Booya Province (KKBP), which was reworked during the Proterozoic, represents the margin of the Archean Yilgarn Craton that was reworked by Proterozoic magmatism (Kirkland et al., 2016a). Four fault-bounded tectonostratigraphic units comprise the KKBP—the Tropicana, Biranup, Nornalup and Fraser Zones (Fig. 1).

The newly-defined Tropicana Zone to the northeast of the AFO contains Neoarchean rocks including the amphibolite to granulite facies Tropicana Gneiss and the Hercules Gneiss (Fig. 1) (Kirkland et al., 2015, Occhipinti et al., 2017). Paleoproterozoic granitic rocks intrude these basement rocks, which in turn are overlain by greenschist to amphibolite facies metasediments of the Lindsay Hill Formation (Barren Basin) (c. 1752 ± 19 Ma) (Occhipinti et al., 2014, Kirkland et al., 2016a). Sanukitoids, low Si, large ion lithophile (LILE)-enriched granites are also found in the Tropicana Zone, and were emplaced during a single event at c. 2692 ± 16 Ma based on zircon U–Pb geochronology (Kirkland et al., 2016a).

The Biranup Zone contains Paleoproterozoic (1800–1620 Ma) basement rocks of dominantly paragneiss and orthogneiss (Spaggiari et al., 2011, Kirkland et al., 2016a), and extends the entire length of the southern and southeastern margin of the Yilgarn Craton (Fig. 1) (Spaggiari et al., 2011). The southernmost and easternmost unit of the Albany–Fraser Orogen is the Nornalup Zone, which is separated from the Biranup Zone by the Heywood–Cheyne Shear Zone (Fig. 1) (Spaggiari et al., 2011). The Nornalup Zone is dominated by Mesoproterozoic intrusions of the Recherche (1330–1280 Ma) and Esperance (1200–1140) Supersuites (Fig. 2) (Nelson et al., 1995, Spaggiari et al., 2011, Smithies et al., 2015). To the north east of the AFO, the Biranup and Nornalup Zones are separated by the Fraser Zone (Fig. 1). The Fraser Zone is comprised of paragneisses (c. 1335 and 1295 Ma) and sheets of interlayered metagabbro and felsic orthogneisses (c. 1290 Ma) (Spaggiari et al., 2011, Clark et al., 2014)

2.2 Tectonomagmatic and metamorphic events

Geochronological evidence, principally zircon U–Pb ages, constrains the main tectonic events of the Albany–Fraser Orogen in the period from 1800 Ma to 1140 Ma (Spaggiari et al., 2011). The evolution of the AFO, and its associated tectonic and metamorphic features, formed as a response to complex and protracted modification of the margin of the Yilgarn Craton through a series of rifting and compressional events (Fig. 2).

2.2.1 Biranup Orogeny

Numerous phases of alkaline granite magmatism during the Paleoproterozoic Biranup Orogeny, resulted in the abundance of syenogranitic rocks in the eastern Biranup Zone (Spaggiari et al., 2011). The Biranup Orogeny occurred shortly after the Salmon Gums (1810–1800 Ma) and Ngadju (1780–1760 Ma) magmatic events (Spaggiari et al., 2011). Thereafter, wide-scale magmatism, the formation of sedimentary basins, and high-temperature metamorphism and deformation during a period from 1710 to 1650 Ma characterise the Biranup Orogeny. Folded leucosomes in a

migmatitic monzogranite record a U–Pb zircon age of 1676 ± 6 Ma, a similar age to cross-cutting axial planar leucosomes (1679 ± 6 Ma) define the newly recognised deformation and high-grade metamorphic event, the Zanthus Event (Fig. 2)(Kirkland et al., 2011).

2.2.2 Albany–Fraser Orogeny

The Mesoproterozoic Albany–Fraser Orogeny is divided into two distinct tectonothermal events: Stage I (1330–1260 Ma) and Stage II (1225–1140 Ma). Stage I was dominated by the emplacement of voluminous mafic to felsic magmas which outcrop prolifically in the Fraser Zone and are also seen widely across the region as the granitic Recherche Supersuite. Emplacement of these c. 1300 Ma magmas was accompanied by deformation and amphibolite to granulite facies metamorphism (Kirkland, 2014, Bodorkos and Clark, 2004a, Bodorkos and Clark, 2004b, Occhipinti et al., 2017, Clark et al., 2000). Stage II of the Orogeny records the development of northwards directed thrusting throughout the Northern Foreland, Biranup and Nornalup Zones, during high-temperature and moderate-pressure metamorphism (Waddell et al., 2015, Occhipinti et al., 2017, Scibiorski et al., 2015).

Changes in tectonic regimes that led to the modification of the Yilgarn margin during the Proterozoic is inferred by the generation of two successive sedimentary basins, named the Barren and Arid Basins (Spaggiari et al., 2015). The Barren Basin (1815–1600 Ma) was filled mainly with Neoproterozoic material principally sourced from the Yilgarn Craton, and Paleoproterozoic material derived from weathering of mostly felsic magmatism associated with the Biranup Orogeny (Spaggiari et al., 2015). The tectonic regime that resulted in the Barren Basin is consistent with formation of a continental rift or a back-arc basin (Spaggiari et al., 2015). Continued extension created a passive margin and oceanic basin along the Yilgarn craton edge, known as the Arid Basin (1600–1305 Ma) (Spaggiari et al., 2015). The Arid Basin contains zircons of c. 1425 – 1375 Ma, a juvenile age which does not correlate with any known sources in the Albany–Fraser Orogen. Furthermore, the Arid Basin is significantly different from the Barren Basin as it records input of exotic source or sources with newly formed crust of different character (Spaggiari et al., 2015).

2.3 Geology of the Fraser Zone

The Fraser Zone is a major component of the eastern part of the Albany–Fraser Orogen, being 425 km long and 50 km wide, and containing the Fraser Range Metamorphics (1305–1290 Ma) (Fig. 1) (Smithies et al., 2013). Although generally unexposed, significant volumes of mafic to ultramafic rocks are interpreted in the Fraser Zone on the basis of gravity data (Brisbourn, 2015). These rocks are bounded to the northwest by the Fraser Shear Zone, and to the southeast by the Newman and

Boonderoo Shear Zones (Fig. 1) (Spaggiari et al., 2011). The Fraser Range Metamorphics comprise a suite of variably thick metagabbroic rocks and metasedimentary rocks that are interleaved with sheets of granitic gneisses of the Recherche and Esperance Supersuites (Spaggiari et al., 2011). The magmatic rocks are best exposed in the southern portion of the Fraser Zone, where they mainly comprise sills that intrude metasedimentary rocks of the Snowys Dam Formation (Smithies et al., 2013, Spaggiari et al., 2014). The southeastern portion of the Fraser Zone is dominated by less deformed and thicker (several centimeters to several hundred meters) metagabbroic sheets, whereas the northwestern half contains tightly to isoclinally-folded, strongly foliated to mylonitic rocks, suggesting significant differences in strain between these two regions (Smithies et al., 2013, Spaggiari et al., 2014).

Metasedimentary and metagranitic rocks of the Fraser Zone contain detrital and xenocrystic zircons with ages consistent with the magmatic rocks that dominate the Biranup Zone (1800–1650 Ma). The presence of 1800–1650 Ma metagranitic rocks, combined with Lu–Hf isotopic data are consistent with reworking of a Biranup source, all suggest that the gabbros and granites of the Fraser Zone were emplaced into the Biranup Zone (Spaggiari et al., 2011, Kirkland, 2014). U–Pb zircon ages and metamorphic overgrowths in metapelitic rocks indicate crystallization of melt at c. 1290 Ma, coincident with the emplacement of mafic rocks at c. 1292 Ma (Clark et al., 2014), suggesting that mafic magmatism was the main thermal driver for granulite facies metamorphism in the Fraser Zone. Counterclockwise P – t paths calculated on pseudosections of metapelitic rocks from the Fraser Zone constrain the peak temperatures to between 800 and 900 °C, and pressures >6.5 kbar (Clark et al., 2014). This relatively rapid heating and near isobaric cooling are consistent with the rocks of the Fraser Zone forming within a back-arc rift setting (Clark et al., 2014). Until recently, there has been no clear evidence for the effects of Stage II (1225–1140 Ma) in the Fraser Zone, despite the close proximity of the Fraser Zone to the Biranup and Nornalup Zones, which contain high-grade Stage II rocks

(Spaggiari et al., 2011). New $^{40}\text{Ar}/^{39}\text{Ar}$ thermochronology (Scibiorski et al., 2016) and U–Pb titanite geochronology (Kirkland et al., 2016b) suggest the Fraser Zone was affected by metamorphism associated with Stage II of the Albany–Fraser Orogeny (Scibiorski et al., 2016). This study focuses on the rocks of the Fraser Zone, specifically the gabbroic and metagabbroic rocks.

3.0 Methods and analytical techniques

3.1 Petrography

The petrographic features of six samples were investigated in thin section using standard transmitted light microscopy with a Leica DC 2000 digital imaging system, a TESCAN Integrated Mineral Analyzer (TIMA) and a MIRA3 Scanning Electron Microscope (SEM). Full thin section photomicrographs were taken using the Zeiss AxioImager.M2m Imaging System. All analyses were conducted at Curtin University. As sample 183654 is a covered thin section, only its petrographic features as observed using standard transmitted light microscopy are described. Samples were provided by the Geological Survey of Western Australia; sample locations are shown in Figure 3 (for full details see Appendix 1).

3.1.1 TESCAN Integrated Mineral Analyzer (TIMA)

The TESCAN Integrated Mineral Analyzer (TIMA) produces a detailed mineralogical characterisation of thin sections using energy-dispersive X-ray spectroscopy, including a measurement of the abundance of all minerals. Samples 216342, 216355, 216350, 183623, 183661 were analysed using the TIMA for an average of 4 hours and 20 minutes per sample. Analyses used a 15.0 mm working distance, a 2500 eV beam intensity and a spot size of 52.29 nm. Results are reported in Tables 1 and 2 (for full details see Appendix 2). TIMA outputs included primary phase maps calculated through energy dispersive spectroscopy (see Appendix 2).

3.1.2 MIRA3SEM and CL Imaging

Zircon analysis was conducted on polished thin sections using the MIRA3 Scanning Electron Microscope (SEM). Backscattered electron (BSE) and cathodoluminescence (CL) images were taken of areas of interest within thin sections to study zircon morphology, internal structure and petrographical relationships. Samples 216342 and 183623 were selected for analysis based on the grain size and abundance of zircon. Samples were carbon coated prior to imaging to prevent charging of the grain surface. CL imaging of zircon grains was conducted using the MIRA3 SEM operating at 12.0 Kv, a working distance of 16.5 mm, and a spot size of 20 nm. Magnification, focus, contrast and brightness were optimised for each sample. Representative grains are shown in Figure 4 and 5.

3.2 XRF major element analysis and Fe-titration

The bulk major element compositions of six samples were measured by X-ray fluorescence (XRF) for the primary purpose of constructing of P – T pseudosections. Chemical analyses were

undertaken at Franklin and Marshall College, Pennsylvania. Representative whole-rock samples were first crushed with a hydraulic press and then milled in a ring and puck agate mill until the powder could pass through a size 8 sieve mesh screen. Whole-rock major trace elements were determined using a Panalytical 2404 XRF instrument. Previously crushed powder ($\sim 0.4 \pm 0.0001$ grams) was mixed with lithium tetraborate (3.6000 ± 0.0002 grams), placed in a platinum crucible and heated using a gas burner until molten. To produce a glass disk for analyses, the molten material was transferred to a platinum casting dish and quenched. The disk was later analysed to establish the concentrations of SiO_2 , Al_2O_3 , CaO , K_2O , P_2O_5 , TiO_2 , total iron (reported as $\text{Fe}_2\text{O}_3\text{T}$), MnO , Na_2O and MgO . Analysis of geochemical rock standards produced working calibration curves for each element (Govindaraju, 1994, Abbey, 1972). Approximately 30–50 data points were gathered for each working curve with various elemental interferences taken into account. The bulk compositions were calculated and presented as weight percent oxides (see Appendix 3). The proportion of FeO and Fe_2O_3 were determined by titration (Reichen and Fahey, 1962). The amount of H_2O was estimated based on loss on ignition by heating an exact aliquot of the sample at 950°C for a total of one hour.

3.3 Pseudosections

Pseudosections were calculated based on the major element bulk compositions (XRF) of samples to investigate the pressure–temperature evolution of rocks. Calculations were performed using THERMOCALC 3.33i (Powell and Holland, 1985) in the system $\text{Na}_2\text{O}–\text{CaO}–\text{K}_2\text{O}–\text{FeO}–\text{MgO}–\text{Al}_2\text{O}_3–\text{SiO}_2–\text{H}_2\text{O}–\text{TiO}_2–\text{Fe}_2\text{O}_3$ (NCKFMASHTO) for metamorphosed samples (183621, 183661, 183654) that contain hydrous minerals (mainly hornblende) interpreted to form part of the peak assemblage, and NCKFMASHTO for magmatic samples 216342, 216355, 216350, which contain no peak hydrous minerals. Following (Kretz, 1983), mineral abbreviations are as follows: Ap – apatite; Bt – biotite; Cpx – clinopyroxene; Di – diopside; Grt – garnet; Hem – hematite; Hbl – hornblende; Ilm – ilmenite; Kfs – K-feldspar; Liq – liquid; Mag – magnetite; Ms – muscovite; Ol – olivine; Opx – orthopyroxene; Pn – pentlandite; Pl – plagioclase; Py – pyrite; Po – pyrrhotite; Qtz – quartz; Rt – rutile. Interpreted peak mineral assemblages were identified based on petrographic observations (outlined in section 3.1 and Appendix 4); the appropriate peak fields are indicated in the pseudosections (Fig. 6–7).

3.4 Geochronology and trace element geochemistry

Zircon targets for age U–Pb dating were identified based on both backscattered electron (BSE) images and TIMA phase maps. Elemental and isotopic data was determined using Laser Ablation

Multi-Collector Inductively-Coupled Plasma Mass Spectrometry (LA-MC-ICPMS) at the GeoHistory Facility in the John de Laeter Centre, Curtin University. Individual zircon grains within polished thin sections 216342 and 183623 were ablated using a Resonetics RESolution M-50A-LR system, comprising a Compex 102-193 nm excimer UV laser with a 23 μm diameter laser spot, attenuation value of 26%, laser repetition rate of 5 Hz and laser energy of 1.81 cm^2 . U-Pb isotopic intensities were measured using a Nu Plasma II multicollector ICP-MS, using 91500 as the primary standard and GJ1 /Plesovice as secondary standards. GJ1 and Plesovice standards yield a weighted average age of 604.3 ± 3.4 Ma (2σ MSWD = 1.8) and 341.7 ± 20 Ma (2σ MSWD = 1.9) respectively. Trace element intensities were measured concurrently using an Agilent 7700 series quadrupole-ICP-MS. Primary GJ1 and secondary NIST612 standards were used for trace element analyses. Analyses 216342 -1 to 216342-13 (spot numbers 1-13) were obtained from magmatic sample 216342 and Analyses 183623-2 to 183623-12 (spot numbers M1 –M12) were obtained from metamorphic sample 183623. Refer to Figure 4 and 5 for exact spot locations.

Both trace element and U-Pb data were processed in the program Lolite using the appropriate reduction schemes. A summary of the LA-MC-ICPMS data and trace element geochemistry are given in Appendix 5 and 6.

4.0 Petrographic observations

Three gabbroic and three metagabbroic samples from the Fraser Zone were analysed in detail. The primary magmatic samples show little or no evidence of subsequent metamorphism. The metagabbros are weakly foliated, and are characterised by two-pyroxene granulite facies assemblages containing peak metamorphic hornblende. Detailed petrographic descriptions, including mineral abundances (TIMA) for all samples are given below.

4.1 Magmatic samples

In general, all magmatic samples contain clinopyroxene, orthopyroxene, plagioclase, biotite, ilmenite and quartz (Table 1) with minor magnetite, zircon, ilmenite, pyrrhotite, apatite, pyrite, pentlandite and chalcopyrite (see Appendix 2). Clinopyroxene occurs as pale green subhedral grains with an average size of 0.5 mm and is also found as inclusions within orthopyroxene.

Orthopyroxene (1–2 mm) is morphologically similar to, and generally more abundant than, clinopyroxene. Both pyroxenes exhibit distinct exsolution of ilmenite platelets, a feature that is more common in the coarser-grained samples (216342 and 216355, Fig. 8, a-b). Plagioclase (1 – 2 mm) forms subhedral laths and is commonly partially sericitised. Granular quartz (0.5 mm) occurs

in samples 216350 and 216355 and shows undulose extinction. Biotite forms subhedral prismatic grains on average 0.5 mm in length. Ilmenite is the main opaque phase in all samples and has a maximum size of ~4 mm. Other opaque phases (~0.2 mm) such as magnetite are generally developed along grain boundaries, in the interstices between grains and as inclusions. Individual samples are described below:

4.1.1 Sample 216342

Sample 216342 is a medium-grained rock containing orthopyroxene, clinopyroxene, plagioclase, biotite and minor orthoclase and muscovite. Accessory minerals include ilmenite, pyrrhotite, apatite, pentlandite, pyrite, chalcopyrite, rutile, zircon, hematite/magnetite and calcite. Orthopyroxene comprises ~55 – 60 vol.% of the sample and commonly forms subhedral grains with an average diameter of ~2 mm, distinguishable from clinopyroxene by its pale pink to pale green pleochroism. Clinopyroxene comprises ~5 vol.% and has an average diameter of ~1 mm. Both pyroxenes show distinct oriented exsolution of ilmenite platelets, which occur both within grain cores and rims. Subhedral biotite (~5 vol.%; on average 0.4 mm long) mainly forms at the margins of, and as inclusions within, pyroxene grains. Plagioclase (~30 vol.%) is anhedral to subhedral with an average grain size of 2 mm and some grains show sericitic alteration. Quartz (~2 vol.%) is mostly anhedral, shows undulose extinction and has a maximum grain size of 1 mm. Ilmenite, magnetite and rutile together comprise ~1 vol.%. Elongate opaque minerals with an average size of ~4 mm fill the gaps between pyroxene grains. Distinctively smaller (~0.4 mm) anhedral opaque blebs form at the margins of, and as inclusions within, biotite and pyroxenes. Anhedral prismatic rutile grains occur on the grain boundaries of pyroxene (~0.4 mm). A discontinuous corona of zircon crystals (~25 μm) surrounding ilmenite is observed (Fig. 4, a). The interpreted primary magmatic assemblage in sample 216342 is orthopyroxene, clinopyroxene, plagioclase, orthoclase, quartz, and ilmenite (Fig. 8, a).

4.1.2 Sample 216355

Sample 216355 is a medium-grained rock containing clinopyroxene, orthopyroxene, plagioclase, biotite and minor orthoclase and muscovite. Accessory minerals include ilmenite, pyrrhotite, apatite, pentlandite, pyrite, chalcopyrite, rutile, zircon, hematite/magnetite and calcite. Clinopyroxene comprises ~15–20 vol.% of the sample and commonly forms pale green subhedral grains with an average diameter of ~1 mm. Orthopyroxene (~20 vol.%; on average 1.5 mm across) is morphologically similar to clinopyroxene and shows distinct characteristic pale pink to pale green pleochroism. Some orthopyroxene grains contain exsolution lamellae of clinopyroxene.

Both pyroxenes contain inclusions of biotite and oriented platelets of exsolved ilmenite. Subhedral biotite (~1 vol.%; on average 0.4 mm long) mainly forms at the margins of pyroxene grains. Plagioclase (~55–60 vol.%) is euhedral to subhedral with an average grain size of 1.5 mm. Quartz (<2 vol.%) is mostly subhedral, shows undulose extinction and has a maximum grain size of 1.5 mm. Elongate ilmenite (<2 vol.%) is associated with biotite and forms subhedral grains that are on average 0.5 mm across. The interpreted primary magmatic assemblage in sample 216355 is orthopyroxene, clinopyroxene, plagioclase, quartz and ilmenite (Fig. 8, b).

4.1.3 Sample 216350

Sample 216350 is a fine-grained rock containing orthopyroxene, clinopyroxene, plagioclase, biotite, quartz and minor orthoclase, muscovite, calcite and kaolinite. Opaque minerals include ilmenite, magnetite, pyrrhotite, apatite, pyrite, chalcopyrite and pentlandite. Clinopyroxene comprises ~20–25 vol.% of the sample and commonly forms anhedral to subhedral grains with an average diameter of ~1 mm. Orthopyroxene comprises ~20–25 vol.% and has an average diameter of ~1 mm. Both pyroxenes show distinct oriented exsolved ilmenite platelets, although these are notably less abundant than in samples 216342 and 216335. Elongate, subhedral biotite (~1 vol.%; on average 0.4 mm long) forms along grain boundaries of plagioclase and pyroxene grains. Plagioclase (~50–55 vol.%) forms subhedral laths with an average grain size of ~1 mm and is commonly partially sericitised. Anhedral quartz with distinct undulose extinction comprises < 5 vol. % of the sample. Anhedral opaque magnetite blebs (~1 mm; ~2 vol.%), form on the grain boundaries and as inclusions within biotite and pyroxenes. Elongate opaque ilmenite is present on pyroxene grain boundaries (~1.5 mm; ~1vol.%). The interpreted primary magmatic assemblage in sample 216350 is orthopyroxene, clinopyroxene, plagioclase, quartz and ilmenite (Fig. 8, c).

4.2 Metamorphic samples

In general, samples of the metamorphosed gabbros contain clinopyroxene, orthopyroxene, hornblende, biotite, plagioclase, quartz (Table 2), minor ilmenite and accessory minerals including apatite, calcite, hematite, magnetite and pyrrhotite. In most cases, clinopyroxene forms pale green subhedral grains with an average diameter of ~1.5mm. Orthopyroxene is morphologically similar to clinopyroxene, and shows distinct pale green to pale pink pleochroism, and is significantly more abundant than clinopyroxene in all samples. A continuous foliation present in all samples is defined by the alignment of hornblende and/or biotite grains. Hornblende occurs as prismatic grains which are on average ~1 mm in diameter. Ilmenite and magnetite are the main opaque phases in both samples analysed by TIMA. Ilmenite commonly forms elongate grains and

magnetite occurs as anhedral blebs. Anhedral pyrrhotite is found only in sample 183623 spatially associated with magnetite. Individual samples are described below:

4.2.1 Sample 183623

Sample 183623 is a medium-grained foliated rock containing clinopyroxene, orthopyroxene, hornblende, biotite, plagioclase, quartz and minor orthoclase and muscovite. Accessory minerals include ilmenite, apatite, hematite/magnetite, pyrrhotite and zircon. Clinopyroxene comprises ~10 vol.% of the sample and commonly forms pale green subhedral grains with an average diameter of ~1 mm. Orthopyroxene (~20–25 vol.%; on average 1 mm across) is morphologically similar to clinopyroxene and shows distinct pale pink to pale green pleochroism. Hornblende (15 vol.%) forms brown, subhedral, elongate to prismatic grains which are on average ~1 mm across that, together with subhedral, elongate laths of biotite (~2 vol.%, on average ~0.5 mm), define a continuous foliation. Secondary biotite is also present within fractures in pyroxene grains. Plagioclase (0.5 – 1 mm) is subhedral, exhibits complex compositional zoning and comprises ~50% of the sample. Quartz (~1–2 vol.%, and on average 0.5 mm) is granoblastic and exhibits undulose extinction. Ilmenite and opaque phases such as magnetite (~2 vol.%) occur as anhedral to elongate grains clustered along grain boundaries of hornblende and biotite. The interpreted peak assemblage in sample 183623 is orthopyroxene, clinopyroxene, hornblende, plagioclase, ilmenite and melt. Biotite in this sample is present as a primary mineral and also as a secondary replacement and therefore biotite has been included in the peak assemblage (Fig. 8, d).

4.2.2 Sample 183661

Sample 183661 is a medium-grained, foliated rock containing clinopyroxene, orthopyroxene, hornblende, plagioclase, quartz and minor orthoclase, calcite and muscovite. Accessory minerals include ilmenite, apatite, hematite/magnetite, garnet and zircon. Clinopyroxene forms subhedral pale green grains that are on average ~1 mm across and comprise ~15 vol.% of the sample. Orthopyroxene (~20 –25 vol.%) shows distinct pink to pale green pleochroism and is morphologically similar to clinopyroxene. A continuous foliation is defined by elongate, subhedral, pleochroic yellow to brown hornblende (~15–20 vol.%). The maximum length of hornblende grains is ~1.5 mm and hornblende commonly shows dark oriented exsolution lamellae of clinopyroxene. Plagioclase is volumetrically dominant, comprising between 45 and 50 vol.% of the sample. Most grains form subhedral laths that are on average ~1 mm in length and commonly show signs of alteration to sericite within fractures. Quartz (~2 vol.%; on average 0.5–1 mm across) is granoblastic and exhibits undulose extinction. Ilmenite and other opaque minerals (2 vol.%) have a

maximum length of ~1 mm, are commonly elongated subparallel to the foliation and occur along grain boundaries, within the matrix and as inclusions in pyroxene and hornblende. Hexagonal apatite grains (~100 microns; 0.4 vol.%) are evident as inclusions within plagioclase grains. The interpreted peak assemblage in sample 183661 is orthopyroxene, clinopyroxene, hornblende, plagioclase, ilmenite and melt (Fig. 8, e). Biotite in this sample is only present as a secondary replacement.

4.2.3 Sample 183654

Sample 183654 is a medium-grained rock containing clinopyroxene, orthopyroxene, olivine, hornblende, biotite, plagioclase and minor opaque phases including ilmenite and hematite/magnetite. Clinopyroxene (~15 vol.%) forms subhedral grains that are on average ~1 mm in length and which is distinguishable from orthopyroxene due to the common development of twinning. Orthopyroxene comprises ~20 vol.% of the sample. Grains are on average ~1 mm across, show distinct pale green to pale pink pleochroism and contain inclusions of plagioclase and hornblende. Olivine forms subhedral grains with distinct uneven fractures, comprises ~10 vol.% of the sample. Commonly olivine grains are spatially associated with pyroxenes and show alteration to green serpentine localised along fractures. Hornblende (~20 vol.%) shows pale cream to dark brown pleochroism, prismatic shapes; grains are on average ~1 mm long. Plagioclase forms subhedral laths on average ~1 mm in size and comprises ~30 vol.% of the sample. Minor biotite (~2 vol.%) and opaque minerals (~5 vol.%) occur throughout the sample. Anhedral opaque minerals cluster on grain boundaries, in the interstices between pyroxene and plagioclase, and as inclusions within hornblende and plagioclase. The interpreted peak assemblage in sample 183654 is olivine, orthopyroxene, clinopyroxene, hornblende, plagioclase, ilmenite and melt (Fig. 8, f). Biotite in this sample is only present as a secondary replacement.

5.0 Mineral equilibria modelling

Mineral equilibria modelling was undertaken to constrain the conditions of metamorphism in the Fraser Zone and to compare and contrast these with recent findings by Clark et al., (2014) using metapelitic rocks from the Fraser Zone.

5.1 Magmatic Samples

Sample 216342 contains an interpreted primary magmatic assemblage of orthopyroxene, clinopyroxene, plagioclase, orthoclase, quartz and ilmenite. The absence of rutile and garnet in this sample helps to constrain conditions to ~10.5 kbar and 960 °C respectively (Fig. 6, a).

Sample 216355 contains an interpreted primary magmatic assemblage of orthopyroxene, clinopyroxene, plagioclase, quartz and ilmenite. This assemblage is predicted to be stable at temperatures between 920 and 1050 °C and pressures lower than 6.8 kbar (highlighted in Fig. 6, b). The absence of orthoclase in the sample constrains the minimum temperature to 920 °C. The lack of rutile constrains the upper pressure limits to ~ 6.8 kbar.

The interpreted primary magmatic assemblage in 216350 includes orthopyroxene, clinopyroxene, plagioclase, quartz and ilmenite (Fig. 6, c). As with sample 216355 the absence of peak orthoclase constrains the minimum temperature to 955 °C. The lack of garnet and rutile within this sample places an upper pressure limit of ~11 kbar.

5.2 Metamorphic Samples

Sample 183623 contains an interpreted peak assemblage of orthopyroxene, clinopyroxene, hornblende, plagioclase, biotite, ilmenite and melt. Based on the constructed pseudosection, this peak assemblage is predicted to be stable at temperatures greater than 850 °C and pressures exceeding ~ 10 kbar (Fig. 7, a). Biotite in this sample is present as both a primary phase and replacement texture, for this reason it has been included in the peak assemblage. Sample 183661 contains an interpreted peak assemblage of orthopyroxene, clinopyroxene, hornblende, plagioclase, ilmenite and melt. The conditions under which this assemblage is stable is similar to that of sample 183623. The absence of garnet and lack of primary biotite constrain the minimum pressure–temperature conditions to ~9 kbar and 825 °C respectively (Fig. 7, b). The interpreted peak assemblage includes olivine, orthopyroxene, clinopyroxene, hornblende, plagioclase and ilmenite. Absence of garnet, lack of primary biotite and insufficient evidence of presence of melt indicates that this peak assemblage is stable at temperatures between 820 – 1020 °C and pressures lower than ~8 kbar (Fig. 7, c).

6.0 U–Pb zircon geochronology

Twenty-five analyses were obtained from seven zircon crystals within magmatic sample 216342 and metamorphic sample 183623. Of the 25 analyses, 3 displayed >10% discordance, interpreted to record post crystallisation disturbance, and are not considered further. *In situ* U–Pb zircon analyses for samples 216342 and 183623 yield concordia ages of 1295.5 ± 4.9 Ma (2σ , MSWD = 1.3) and 1293.0 ± 5.7 Ma (2σ , MSWD = 1.4) respectively (Fig. 9).

6.1 Sample 216342

Sample 216342 is a medium-grained gabbroic rock which displays primary magmatic texture from the south – south east of the Fraser Zone. Zircons from this sample are subhedral to prismatic, up to ~30 μm long and are dusty pale brown. Additionally, some zircon crystals display a specific habit in which they are located in contact with ilmenite or more rarely apatite, forming along grain boundaries in a discontinuous corona (Fig. 4). CL images display fine oscillatory zoning (Fig. 4). Thirteen analyses yield a concordia age of 1295.5 ± 4.9 Ma (2σ , MSWD = 1.3) (Fig 9, a). See Appendix 5 for more data.

6.2 Sample 183623

Sample 183623 is a medium-grained, weakly foliated gabbroic rock from the south-south west of the Fraser Zone. Zircons from this sample vary between anhedral to elongate prisms (Fig. 5), up to ~80 μm long and are dusty pale brown. CL images display fine to medium oscillatory zoning and a bright CL response resorption line with variable thickness (Fig. 5). Four analyses >6% discordant are not considered further, including a single inherited grain with an age of 2660 ± 130 Ma. Twelve analyses yield a concordia age of 1293.0 ± 5.7 Ma (2σ , MSWD = 1.4).

6.3 Zircon trace element geochemistry

Figure 10 presents the zircon REE data in spider diagrams for both magmatic sample 216342 (Fig. 10, a) and metamorphic sample 183623 (Fig. 10, b). One distinct REE profile can be recognised in both samples and can be associated with a similar growth process. A steep positive slope La to Lu is observed, where there is a high concentration towards Heavy Rare Earth Elements (HREE), a strong depletion in La and Pr and a weak Ce anomaly.

7.0 Discussion

7.1 Metamorphic evolution of the Fraser Zone

Granitic, mafic and ultramafic rocks of the Fraser Zone are interpreted to have Mesoproterozoic intrusion ages between 1310 and 1283 Ma (Kirkland, 2014, Clark et al., 2014). Granulite facies metamorphism is interpreted to have occurred between 1285 and 1268 Ma. The style of metamorphism documented in these rocks requires an initial period of high-temperature metamorphism consistent with a high geothermal gradient (≥ 800 °C/ 6 to 7 kbar) followed by near isobaric cooling (Clark et al., 1999, Clarke et al., 1995, Spaggiari et al., 2011). A summary of SHRIMP U–Pb data presented in Clark et al., (2014) illustrates the coeval nature of mafic and

granitic magmatism and metamorphism within the Fraser Zone and suggests that magmatism was the thermal driver for granulite facies metamorphism. The results in this study are consistent with these earlier findings.

Magmatic gabbros in this study, contain near anhydrous primary magmatic assemblages dominated by orthopyroxene, plagioclase and clinopyroxene. Hydrated metagabbroic rocks contain peak metamorphic mineral assemblages dominated by plagioclase, orthopyroxene, hornblende and clinopyroxene. Based on the results of phase equilibria modelling, the primary magmatic assemblages are consistent with equilibration temperatures of $\sim 950^\circ\text{C}$, which likely record final crystallisation of the last vestiges of melt. The peak assemblages within the metamorphic samples are similarly consistent with high temperatures of $\sim 900^\circ\text{C}$. These conditions are summarised in Figure 11, which shows a combination of the six calculated pseudosections. The interpreted fields have overlapping fields that constrain temperature to around 950°C . Based on the absence of garnet, pressures experienced by the gabbroic rocks are equal to or below 7 kbar.

Studies of the Fraser Zone rocks by Clark et al., (1999) and Clark et al., (1995) recognised two episodes of metamorphism—a granulite facies ($830\text{--}860^\circ\text{C}$, 6–7 kbar) event at $c.1301 \pm 6$ Ma followed by a higher pressure amphibolite facies event (650°C , 8–10 kbar) at $c. 1293 \pm 9$ Ma and 1288 ± 12 Ma. Based on the six samples modelled in this study, there is no evidence to suggest a second amphibolite facies event. Peak pressures of ~ 7 kbar, documented by Clark et al, (1995) and Clark et al., (1999) for their granulite facies event, and by Clark et al., (2014) are consistent with the data presented here (Fig. 11). However, the (meta) gabbroic rocks record temperatures of $\sim 950^\circ\text{C}$, significantly higher than recorded by the metapelitic rocks ($830\text{--}860^\circ\text{C}$; Clark et al., 2014). This discrepancy reflects the greater distance of the metapelitic source rocks from the magmatic heat source.

7.2 Age interpretation

Geochronological investigations have been abundant in the Fraser Zone. Majority of these analyses use U–Pb isotopic zircon ages and are interpreted igneous crystallisation ages for detrital zircons (Spaggiari et al., 2009, Clark, 1995, Clark et al., 1999). Existing estimates place the timing of intrusion of gabbroic rocks into the Fraser Zone at 1301 ± 6 Ma, based on zircon within a charnockite (Clark et al., 1999). Clark et al., (1999) identified a $^{207}\text{Pb}/^{206}\text{Pb}$ age of 1305 ± 80 Ma from zircons rims formed during high grade metamorphism. Metamorphic rims on zircon grains from a metasandstone recorded an age of 1304 ± 7 Ma. More recent studies by Clark et al., (2014)

yielded a $^{207}\text{Pb}/^{235}\text{U}$ monazite age of 1268 ± 12 Ma from monazites occurring both as inclusions within garnet and in the matrix, which was interpreted to date metamorphism. Such similar ages imply short lived metamorphism, and support the interpretation that the Fraser Zone did not undergo two distinct events (Clark et al., 2014, Foster et al., 2000).

Textural features of zircon crystals in magmatic sample 216342 are variable. Medium to fine oscillatory zoning and triple junction grain boundaries lead to an interpretation that the concordia age of 1295.5 ± 4.9 Ma (2σ , MSWD = 1.3) dates crystallisation of the gabbro (Fig. 4). This age is similar to the intrusive age for a charnockite (1301 ± 6 Ma; (Clark et al., 1999). The concordia age of gabbro crystallisation in this study is similar to a U/Pb zircon age of c. 1291 ± 8 Ma reported by De Waele and Pisarevsky (2008) from mafic granulites within the Fraser Zone. Additionally, a discontinuous zircon corona surrounding an ilmenite grain is observed in magmatic sample 216342 (Fig. 4, a-e). These zircons are interpreted to have occurred during diffusion as the magmatic gabbro slowly cooled.

There is a clear boundary between core and surrounding over growth region in zircons from metamorphic sample 183623. A bright CL response resorption line with irregular thickness marks the dissolution front in the inherited zircon. This bright CL feature represents the boundary between the inherited zircon and the metamorphic overgrowth (Fig. 5). This suggest that zircons from sample 183623 formed during metamorphism and the concordia age of 1293.0 ± 5.7 Ma (2σ , MSWD = 1.4) is the age of metamorphism, consistent with the existing estimates (c. 1290 Ma) (Clark et al., 2014). The single inherited grain of Archean age (c. 2660 ± 130 Ma) (Fig. 5, spot 9) is consist with the bulk of material in the Yilgarn Craton.

7.3 Zircon

Despite the fact that zircons are less common in mafic rocks, distinctive zircon rims around ilmenite grains have been observed in a variety of mafic plutonic rocks such as: anorthosite, Fe–Ti oxide ores (Morisset and Scoates, 2008) and in this study, magmatic gabbro.

The formation of zircons rims around ilmenite grains requires a reaction between the diffused zirconium (Zr) with silica to form zircon (ZrSiO_4). In magmatic sample 216342, it is clear that zircon rims do occur adjacently to silicate minerals (e.g. plagioclase, hornblende), which could have contributed to the silica required for the reaction. Additionally, as shown in previous literature, it may be possible that the presence of a high-temperature aqueous fluid helped to mobilise Zr from ilmenite by a dissolution-reprecipitation mechanism (Dymek and Schiffries, 1987). A vermicular

intergrowth of quartz and plagioclase, thought to have formed as a reaction between intercumulus plagioclase and high-temperature aqueous fluid is evidence of dissolution-reprecipitation (Dymek and Schiffries, 1987). The partial dissolution of ilmenite, which may have been allowed by locally derived aqueous fluid, may have enabled the liberation of Zr, which could react with silica to form ZrSiO_4 (zircon). Common characteristics of this dissolution-reprecipitation process include: porous rim around ilmenite grain or chemical zoning between the core of unreacted ilmenite and reacted rim (Putnis, 2002, Morisset and Scoates, 2008). In addition, it has been shown that REE patterns for zircons formed by hydrothermal fluid show distinct flat LREE patterns, and a subdued flattening of the HREE profile from Dy to Lu (Kirkland et al., 2009). Figure 10 highlights the REE patterns of zircons within the Fraser Zone gabbros, no evidence of flat LREE patterns or a flattening of HREE is observed. The magmatic samples in this study show no evidence of these textural features or REE profiles, and are therefore interpreted to have no association with hydrothermal fluids.

The crystallographic lattice of ilmenite is advantageous to the chemical diffusion of Zr on grain margins (Morisset and Scoates, 2008). Ilmenite ($\text{Fe}^{+2}\text{Ti}^{+4}\text{O}_3$) consists of stacked layers of oxygen octahedra, the Fe^{+2} and Ti^{+4} ions occupy alternating layers (Lindsley, 1976). Zirconium and titanium are both found in group 4 of the Periodic table, have similar chemical properties and are considered relatively immobile trace elements (Perez et al., 2003). These similar properties enable cations of Zr^{+4} to potentially migrate along the layers of Ti^{+4} in ilmenite through a series of 'jumps', relocating to equivalent sites within each layer (Morisset and Scoates, 2008). Diffusion, an important phenomenon in earth systems, contributes to chemical transport and exchange. Diffusion is temperature dependent and for this reason the diffusion of Zr in ilmenite would be increased at high temperatures (e.g., $\sim 1000^\circ\text{C}$ down to 750°C) (Watson and Baxter, 2007). Slowly cooled gabbroic rocks of the Fraser Zone exhibit zircon rims around ilmenite grains. Therefore, the diffusion of Zr from ilmenite could provide cations for zircon formation along grain boundaries of ilmenite. In addition, zircon REE data from sample 216342 (Fig. 10) shows a steep positive La to Lu slope, interpreted to reflect igneous zircons crystallised from a silicate melt (Kirkland et al., 2009). High temperatures experienced by magmatic gabbros ($\sim 950^\circ\text{C}$) and magmatic zircon REE profiles prompt the interpretation of zircon corona around ilmenite to have formed via diffusion.

8.0 Conclusions

The recent development of thermodynamic solution models pertaining to high-temperature phase equilibria in mafic systems permits consideration of the crystallisation depths of mafic magmas as well as the subsequent metamorphism and partial melting of the crystallised mafic rocks. This study presents new phase equilibria modelling of gabbroic and metagabbroic rocks from the Fraser Zone. Pressure constraints from the (meta) gabbros of around 7 kbar are similar to those derived using metapelitic rocks, consistent with depths for both of around 20–25 km, assuming no significant tectonic overpressure. However, the (meta) gabbroic rocks record temperatures that are significantly higher ($\sim 950^\circ\text{C}$) compared to those ($\sim 830\text{--}860^\circ\text{C}$) recorded by metapelitic rocks. These higher temperatures suggest closer proximity to the heat source. Geochronological data sets from this study imply that the emplacement of gabbroic rocks at $c.1295.5 \pm 5$ Ma and timing of metamorphism at $c.1293.0 \pm 6$ Ma occurred coevally, supporting the interpretations that the gabbroic rocks provided the heat for metamorphism.

Zircon rims are restricted to the margins of ilmenite in magmatic sample 216342 indicating that the Zr was supplied by the adjacent Ti-based oxide (ilmenite). The origin of zircon rims around ilmenite grains are interpreted to be the result of diffusion of Zr^{+4} along the layers of Ti^{+4} octahedra in ilmenite. Diffusion occurred as the gabbros were emplaced at high temperatures and cooled slowly. The silica required to form the zircon was provided by the adjacent silicate minerals. Based on phase equilibria modelling from this study, this diffusion process is expected to have occurred at similar conditions to those recorded in the magmatic gabbros ($\sim 950^\circ\text{C}$ and $\sim < 10$ kbar). This coronal texture combined with coeval ages of magmatic crystallisation and metamorphism elucidate the prolonged nature of magmatism. These new data, in particular the high-temperature ($\sim 750\text{--}1000^\circ\text{C}$) diffusion process between zircon corona and ilmenite, combined with previous work, suggest that mafic magmatism was the thermal driver for granulite facies metamorphism in the Fraser Zone.

Acknowledgements

I would like to begin by acknowledging all the staff and my fellow peers of the Applied Geology Department at Curtin University who nurtured my passion for geology during the course of my undergraduate degree. Thank you to the Geological Survey of Western Australia who provided funding for this study.

I am grateful to my primary supervisor Tim Johnson for giving me the opportunity to study some fascinating Australian geology. Tim's constant support, enthusiasm and energy has been a great source of motivation during the study. I consider myself lucky to have been able to study under someone so knowledgeable and generous.

Chris Kirkland is thanked for regularly affording me his time to discuss various aspects of geochronology and all things AFO. Chris Clark and Nick Gardiner are thanked for their supervision, and advice throughout the year.

Alex Walker is thanked for his help and of course for introducing some moments of levity. Julian Chard shared his knowledge and assisted greatly with geochronology. A special mention to Michael Hartnady, who was generous with his time and provided unconditional support throughout the year.

Finally, I wish to thank my family and friends, for your love and encouragement.

References

- ABBEY, S. 1972. Standard samples" of silicate rocks and minerals--a review and compilation: Geol. Survey. of Canada Paper, 72-30.
- BODORKOS, S. & CLARK, D. J. 2004a. Evolution of a crustal-scale transpressive shear zone in the Albany–Fraser Orogen, SW Australia: 1. P–T conditions of Mesoproterozoic metamorphism in the Coramup Gneiss. *Journal of Metamorphic Geology*, 22, 691-711.
- BODORKOS, S. & CLARK, D. J. 2004b. Evolution of a crustal-scale transpressive shear zone in the Albany–Fraser Orogen, SW Australia: 2. Tectonic history of the Coramup Gneiss and a kinematic framework for Mesoproterozoic collision of the West Australian and Mawson cratons. *Journal of Metamorphic Geology*, 22, 713-731.
- BRISBOUT, L. 2015. Determining crustal architecture in the east Albany-Fraser Orogen from geological and geophysical data. 152 ed. Geological Survey of Western Australia.
- CLARK, C., KIRKLAND, C. L., SPAGGIARI, C. V., OORSCHOT, C., WINGATE, M. T. D. & TAYLOR, R. J. 2014. Proterozoic granulite formation driven by mafic magmatism: An example from the Fraser Range Metamorphics, Western Australia. *Precambrian Research*, 240, 1-21.
- CLARK, D. J., HENSEN, B. J. & KINNY, P. D. 2000. Geochronological constraints for a two-stage history of the Albany–Fraser Orogen, Western Australia. *Precambrian Research*, 102, 155-183.
- CLARK, D. J., KINNY, P. D. & POST, N. J. 1999. Relationships between magmatism, metamorphism and deformation in the Fraser Complex, Western Australia: constraints from new SHRIMP U–Pb zircon geochronology*. *Australian Journal of Earth Sciences*, 46, 923-932.
- CLARK, W. C. 1995. *Granite petrogenesis, metamorphism and geochronology of the western Albany-Fraser Orogen, Albany, Western Australia*, School of Applied Geology, Curtin University of Technology.
- CLARKE, G., SUN, S. & WHITE, R. 1995. Grenville-age belts and associated older terranes in Australia and Antarctica. *AGSO Journal of Australian Geology and Geophysics*, 16, 25-40.
- DE WAELE, B. & PISAREVSKY, S. A. 2008. Geochronology, paleomagnetism and magnetic fabric of metamorphic rocks in the northeast Fraser Belt, Western Australia. *Australian Journal of Earth Sciences*, 55, 605-621.
- DYMEK, R. F. & SCHIFFRIES, C. M. 1987. Calcic myrmekite; possible evidence for the involvement of water during the evolution of andesine anorthosite from St-Urbain, Quebec. *The Canadian Mineralogist*, 25, 291-319.
- FOSTER, G., KINNY, P., VANCE, D., PRINCE, C. & HARRIS, N. 2000. The significance of monazite U–Th–Pb age data in metamorphic assemblages; a combined study of monazite and garnet chronometry. *Earth and Planetary Science Letters*, 181, 327-340.
- GOVINDARAJU, K. 1994. 1994 compilation of working values and sample description for 383 geostandards. *Geostandards and Geoanalytical Research*, 18, 1-158.
- KIRKLAND, C., CREASER, R., TESSALINA, S., WATKINS, R., SWEETAPPLE, M. T., WINGATE, M. T. D., SMITHIES, R. & SPAGGIARI, C. 2016a. *Temporal constraints on magmatism, granulite-facies metamorphism, and gold mineralization of the Hercules Gneiss, Tropicana Zone, Albany-Fraser Orogen*.

- KIRKLAND, C., SPAGGIARI, C., JOHNSON, T., SMITHIES, R., DANIŠÍK, M., EVANS, N., WINGATE, M., CLARK, C., SPENCER, C. & MIKUCKI, E. 2016b. Grain size matters: Implications for element and isotopic mobility in titanite. *Precambrian Research*, 278, 283-302.
- KIRKLAND, C. A. S., C. AND SMITHIES, R. AND WINGATE, M 2014. Cryptic progeny of craton margins: geochronology and isotope geology of the Albany–Fraser Orogen, with implications for evolution of the Tropicana Zone. *Albany-Fraser Orogen seismic and magnetotelluric (MT) workshop 2014: extended abstracts (Preliminary edition)*. Geological Survey of Western Australia.
- KIRKLAND, C. L., SPAGGIARI, C. V., PAWLEY, M. J., WINGATE, M. T. D., SMITHIES, R. H., HOWARD, H. M., TYLER, I. M., BELOUSOVA, E. A. & POIJOL, M. 2011. On the edge: U–Pb, Lu–Hf, and Sm–Nd data suggests reworking of the Yilgarn craton margin during formation of the Albany-Fraser Orogen. *Precambrian Research*, 187, 223-247.
- KIRKLAND, C. L., SPAGGIARI, C. V., SMITHIES, R. H., WINGATE, M. T. D., BELOUSOVA, E. A., GRÉAU, Y., SWEETAPPLE, M. T., WATKINS, R., TESSALINA, S. & CREASER, R. 2015. The affinity of Archean crust on the Yilgarn–Albany–Fraser Orogen boundary: Implications for gold mineralisation in the Tropicana Zone. *Precambrian Research*, 266, 260-281.
- KIRKLAND, C. L., WHITEHOUSE, M. J. & SLAGSTAD, T. 2009. Fluid-assisted zircon and monazite growth within a shear zone: a case study from Finnmark, Arctic Norway. *Contributions to Mineralogy and Petrology*, 158, 637-657.
- KRETZ, R. 1983. Symbols for rock-forming minerals. *American mineralogist*, 68, 277-279.
- LINDSLEY, D. 1976. The crystal chemistry and structure of oxide minerals as exemplified by the Fe-Ti oxides. *Oxide minerals*, 3, L1-L60.
- MORISSET, C.-E. & SCOATES, J. S. 2008. Origin of zircon rims around ilmenite in mafic plutonic rocks of Proterozoic anorthosite suites. *The Canadian Mineralogist*, 46, 289-304.
- MORRISSEY, L. J., PAYNE, J. L., HAND, M., CLARK, C., TAYLOR, R., KIRKLAND, C. L. & KYLANDER-CLARK, A. 2017. Linking the Windmill Islands, east Antarctica and the Albany–Fraser Orogen: Insights from U–Pb zircon geochronology and Hf isotopes. *Precambrian Research*, 293, 131-149.
- NELSON, D. R., MYERS, J. S. & NUTMAN, A. P. 1995. Chronology and evolution of the Middle Proterozoic Albany-Fraser Orogen, Western Australia. *Australian Journal of Earth Sciences*, 42, 481-495.
- OCCHIPINTI, S., DOYLE, M., SPAGGIARI, C., KORSCH, R., CANT, G., MARTIN, K., KIRKLAND, C., SAVAGE, J., LESS, T. & BERGIN, L. 2014. Preliminary interpretation of the deep seismic reflection line 12GA-T1: northeastern Albany-Fraser Orogen.
- OCCHIPINTI, S., TYLER, I., SPAGGIARI, C., KORSCH, R., KIRKLAND, C., SMITHIES, R., MARTIN, K. & WINGATE, M. 2017. Tropicana translated: a foreland thrust system imbricate fan setting for c. 2520 Ma orogenic gold mineralization at the northern margin of the Albany–Fraser Orogen, Western Australia. *Geological Society, London, Special Publications*, 453, SP453. 6.
- PEREZ, R. A., NAKAJIMA, H. & DYMENT, F. 2003. Diffusion in α -Ti and Zr. *Materials Transactions*, 44, 2-13.
- POWELL, R. & HOLLAND, T. J. B. 1985. An internally consistent thermodynamic dataset with uncertainties and correlations: 1. Methods and a worked example. *Journal of Metamorphic Geology*, 3, 327-342.

- PUTNIS, A. 2002. Mineral replacement reactions: from macroscopic observations to microscopic mechanisms. *Mineralogical Magazine*, 66, 689-708.
- REICHEN, L. E. & FAHEY, J. J. 1962. improved method for the determination of FeO in rocks and minerals including garnet.
- SCIBIORSKI, E., TOHVER, E. & JOURDAN, F. 2015. Rapid cooling and exhumation in the western part of the Mesoproterozoic Albany-Fraser Orogen, Western Australia. *Precambrian Research*, 265, 232-248.
- SCIBIORSKI, E., TOHVER, E., JOURDAN, F., KIRKLAND, C. L. & SPAGGIARI, C. 2016. Cooling and exhumation along the curved Albany-Fraser orogen, Western Australia. *Lithosphere*, 8, 551.
- SMITHIES, R., SPAGGIARI, C. & KIRKLAND, C. 2015. Building the crust of the Albany-Fraser Orogen: Constraints from granite geochemistry. *GSWA 2015 extended abstracts-promoting the prospectivity of Western Australia*. Geological Survey of Western Australia.
- SMITHIES, R., SPAGGIARI, C., KIRKLAND, C., HOWARD, H. & MAIER, W. 2013. *Petrogenesis of Gabbros of the Mesoproterozoic Fraser Zone: Constraints on the Tectonic Evolution of the Albany-Fraser Orogen*, Geological Survey of Western Australia.
- SPAGGIARI, C., BODORKOS, S., BARQUERO-MOLINA, M., TYLER, I. & WINGATE, M. 2009. Interpreted bedrock geology of the south Yilgarn and central Albany-Fraser orogen, Western Australia. *Geological Survey of Western Australia, Record*, 10, 84.
- SPAGGIARI, C., KIRKLAND, C., PAWLEY, M., SMITHIES, R., WINGATE, M., DOYLE, M., BLENKINSOP, T., CLARK, C., OORSCHOT, C. & FOX, L. 2011. The geology of the east Albany-Fraser Orogen—a field guide. *Geological Survey of Western Australia, Record*, 23, 97.
- SPAGGIARI, C., KIRKLAND, C., SMITHIES, R., OCCHIPINTI, S. & WINGATE, M. Geological framework of the Albany–Fraser Orogen. Albany-Fraser Orogen seismic and magnetotelluric (MT) workshop 2014: Extended abstracts: Geological Survey of Western Australia Volume Record, 2014. 12-27.
- SPAGGIARI, C. V., KIRKLAND, C. L., SMITHIES, R. H., WINGATE, M. T. D. & BELOUSOVA, E. A. 2015. Transformation of an Archean craton margin during Proterozoic basin formation and magmatism: The Albany–Fraser Orogen, Western Australia. *Precambrian Research*, 266, 440-466.
- WADDELL, P.-J. A., TIMMS, N. E., SPAGGIARI, C. V., KIRKLAND, C. L. & WINGATE, M. T. D. 2015. Analysis of the Ragged Basin, Western Australia: Insights into syn-orogenic basin evolution within the Albany–Fraser Orogen. *Precambrian Research*, 261, 166-187.
- WATSON, E. B. & BAXTER, E. F. 2007. Diffusion in solid-Earth systems. *Earth and Planetary Science Letters*, 253, 307-327.

List of figures

Figure 1. Simplified, pre-Mesozoic interpreted bedrock geology of the Albany–Fraser Orogen (modified after (Spaggiari et al., 2009, Kirkland et al., 2011). Abbreviations used: AFO, Albany–Fraser Orogen; MBG, Mount Barren Group; WF Woodline Formation; MRF Mount Ragged Formation. Dotted red box indicates the area in which all samples in this study are located, refer to Fig. 3 for more detailed information.	31
Figure 2. Time-space plot of the Albany–Fraser Orogen and Madura Province, modified from (Spaggiari et al., 2014). Abbreviations used: MRF- Mount Ragged Formation; SDF- Snowys Dam Formation. Question mark indicates uncertainty.....	32
Figure 3. Aeromagnetic image of the south western portion of the Fraser Zone (highlighted in Fig. 1 as a dotted red box). Sample locations are represented by stars.	33
Figure 4. Cathodoluminescence (CL) (a-e) and backscattered electron (f) images of zircon grains in magmatic sample 216342. White spots represent location of analysis and corresponding spot identification numbers are noted next to spot.	34
Figure 5. Cathodoluminescence (CL) (a-d) images of zircon grains in metamorphic sample 183623. White spots represent location of analysis and corresponding spot identification numbers are noted next to spot.	34
Figure 6. Calculated pseudosections for the magmatic samples a) 216342, b) 216355 and c) 216350. Solid black lines represent the crystallisation mineral assemblage for each sample (see Appendix 3 for compositional data).	35
Figure 7. Calculated pseudosections for the metamorphic samples a) 183623, b) 183661 and c) 183654. Solid black lines represent the peak mineral assemblage for each sample (see Appendix 3 for compositional data).....	36

Figure 8. Photomicrographs highlighting the general textures and mineral assemblages observed.

a) magmatic sample 216342, medium grained rock, orthopyroxene, clinopyroxene, plagioclase, orthoclase and ilmenite form the peak assemblage with quartz (not featured) b) magmatic sample 216355, displaying primary igneous layering textures, peak assemblage containing orthopyroxene, clinopyroxene, plagioclase, ilmenite and quartz (not featured). c) magmatic sample 216350, finer grained sample of the magmatic gabbros, contains a peak assemblage of orthopyroxene, clinopyroxene, plagioclase, quartz and ilmenite (latter two not featured here). d) Metamorphic sample 183623, peak assemblage includes orthopyroxene, clinopyroxene, hornblende, plagioclase, ilmenite and melt. e) Metamorphic sample 183661, foliation defined by the alignment of hornblende and biotite, peak assemblage of orthopyroxene, clinopyroxene, hornblende, plagioclase, ilmenite and melt. f) Metamorphic sample 183654, foliated medium grained rock. Foliation defined by prismatic hornblende, olivine crystals show evidence of serpentine alteration. Peak assemblage includes olivine, orthopyroxene, clinopyroxene, hornblende, plagioclase and ilmenite.37

Figure 9. Tera Wasserburg concordia plot of zircon grains analysed by LA-ICP-MS in thin section. a) Zircons analysed in magmatic sample 216342. b) All data from metamorphic zircons, including discordant data. c) All concordant analyses from both magmatic and metamorphic samples. d) Concordant zircon analyses of metamorphic sample 183623. The blue ellipses represent where the all analyses overlap each other.....38

Figure 10. REE composition of zircons within magmatic gabbro (216342) (a) and from metamorphosed gabbro (183623) (b) from the Fraser Zone, WA. Normalised to CL Chondrite.39

Figure 11. Compilation of pseduosections from the gabbroic rocks of the Fraser Zone, constraining the peak conditions of these rocks in the area. Green box represents the already constrained conditions of the metapelites of the Fraser Range Metamorphics from Clark et al., (2014). White star is the inferred peak crystallisation/metamorphic conditions recorded by the (meta) gabbroic rocks studied in this paper.40

List of tables

Table 1. Main mineral percentage compositions of the magmatic gabbroic samples; 216350, 216355 and 216342. These percentages are approximate and were compiled using TESCANA Integrated Mineral Analyser and optical petrology data.....	41
Table 2. Main mineral percentage compositions of the metamorphic gabbroic samples; 183623 and 183661. These percentages are approximate and were compiled using TESCANA Integrated Mineral Analyser and optical petrology data.	41

List of appendices

Appendix 1: Details of sample locations

Appendix 2: TESCAN Integrated Mineral Analyser results

Appendix 3: XRF results

Appendix 4: Detailed petrographic descriptions

Appendix 5: U–Pb geochronology data

Appendix 6: Trace element geochemistry data

Figures

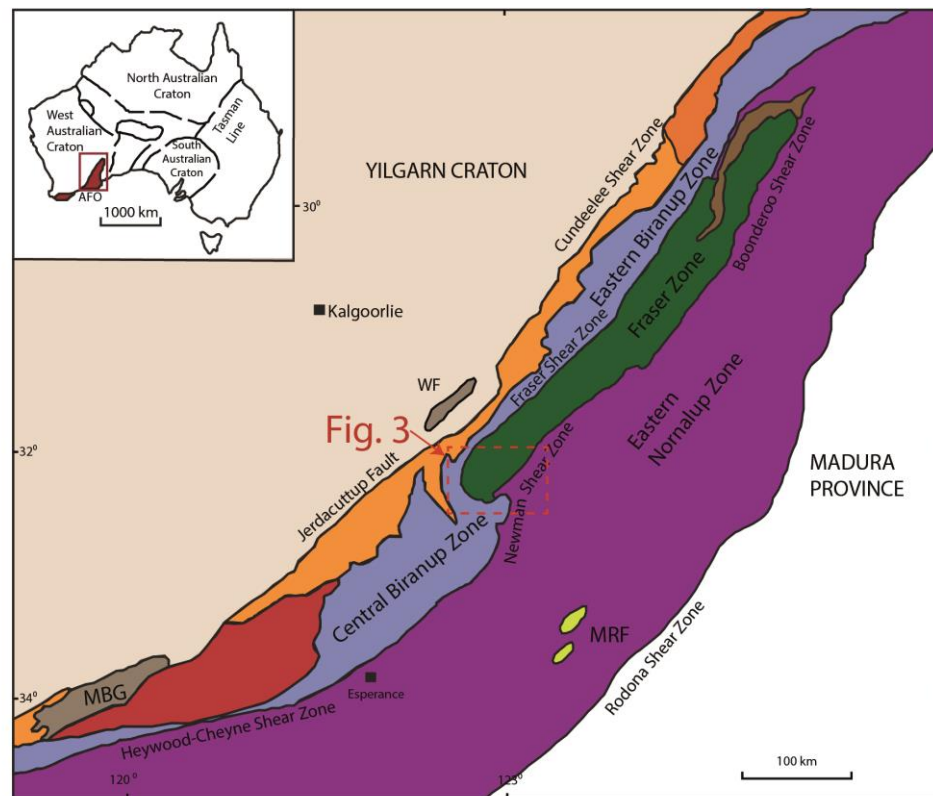
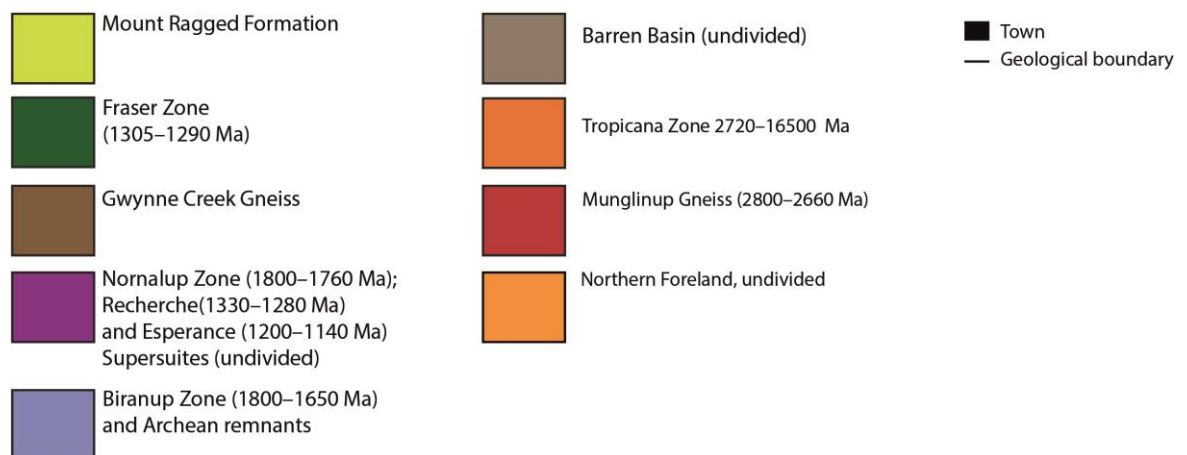
**Albany-Fraser Orogen**

Figure 1. Simplified, pre-Mesozoic interpreted bedrock geology of the Albany–Fraser Orogen (modified after (Spaggiari et al., 2009, Kirkland et al., 2011). Abbreviations used: AFO, Albany–Fraser Orogen; MBG, Mount Barren Group; WF Woodline Formation; MRF Mount Ragged Formation. Dotted red box indicates the area in which all samples in this study are located, refer to Fig. 3 for more detailed information.

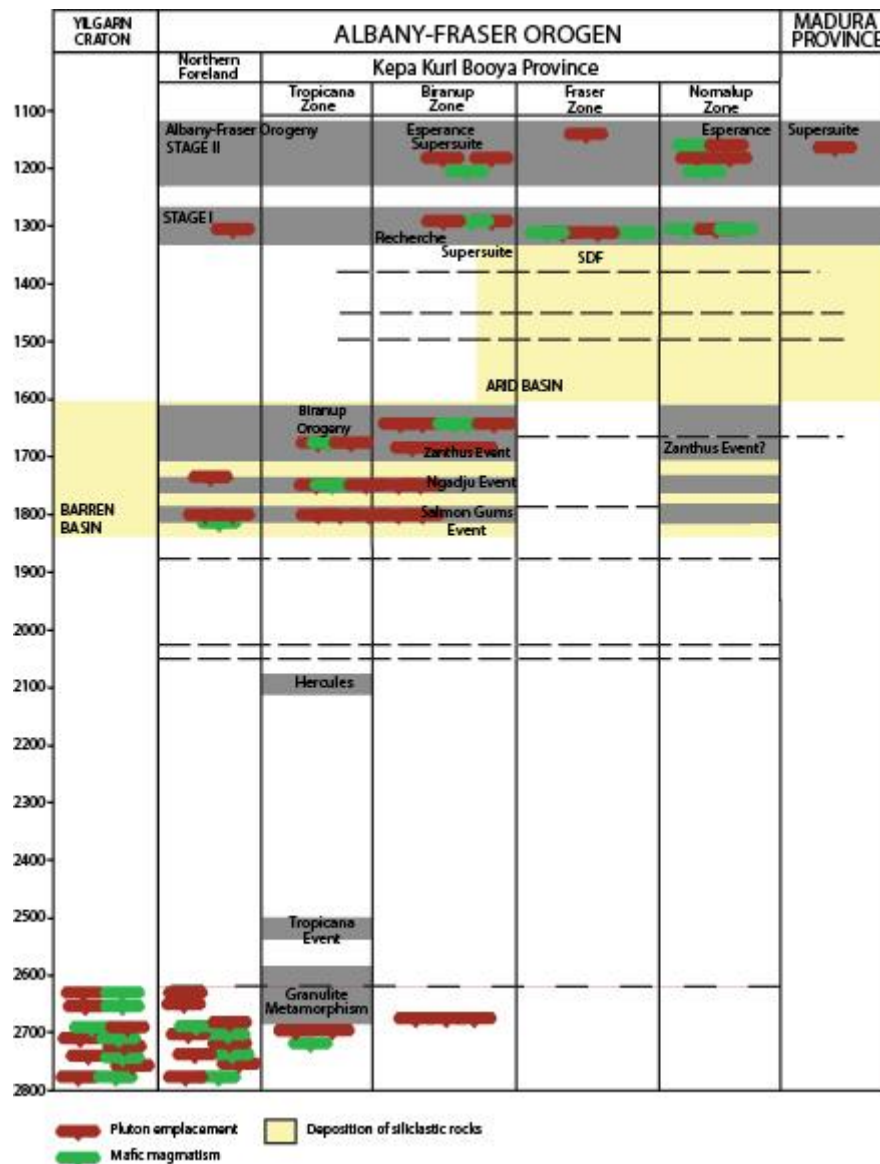


Figure 2. Time-space plot of the Albany–Fraser Orogen and Madura Province, modified from (Spaggiari et al., 2014). Abbreviations used: MRF- Mount Ragged Formation; SDF- Snowys Dam Formation. Question mark indicates uncertainty.

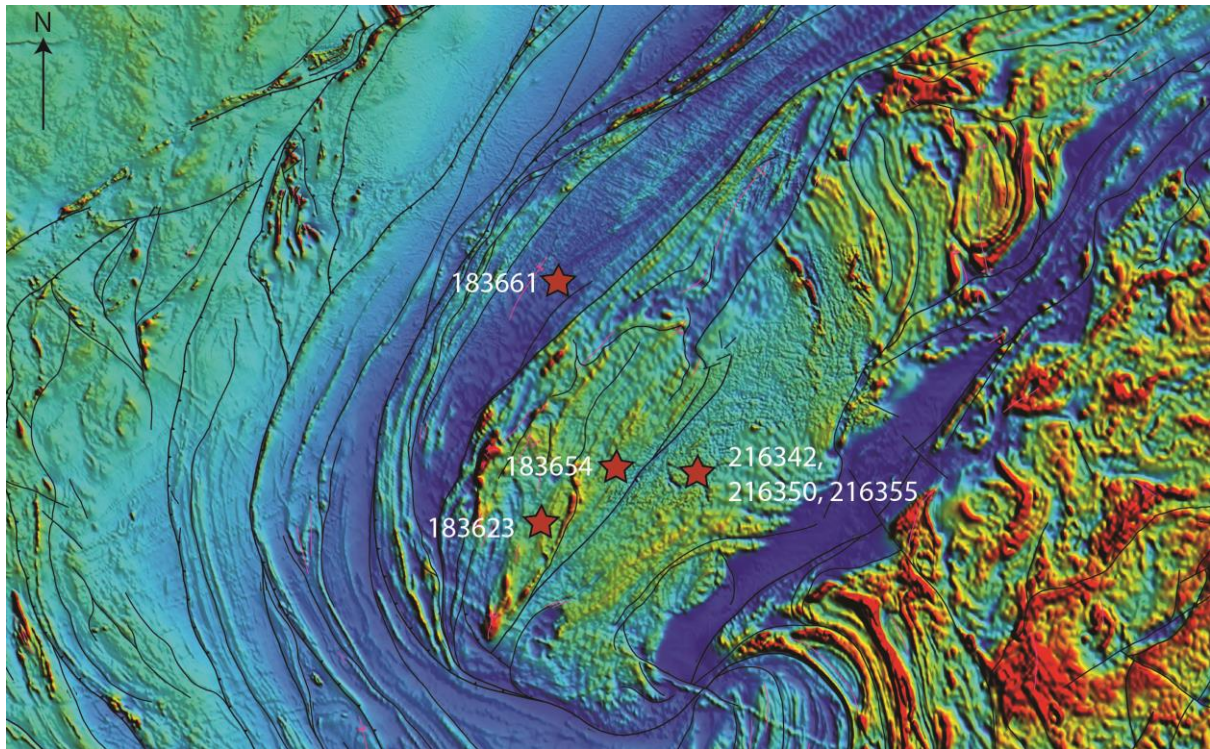


Figure 3. Aeromagnetic image of the south western portion of the Fraser Zone (highlighted in Fig. 1 as a dotted red box). Sample locations are represented by stars.

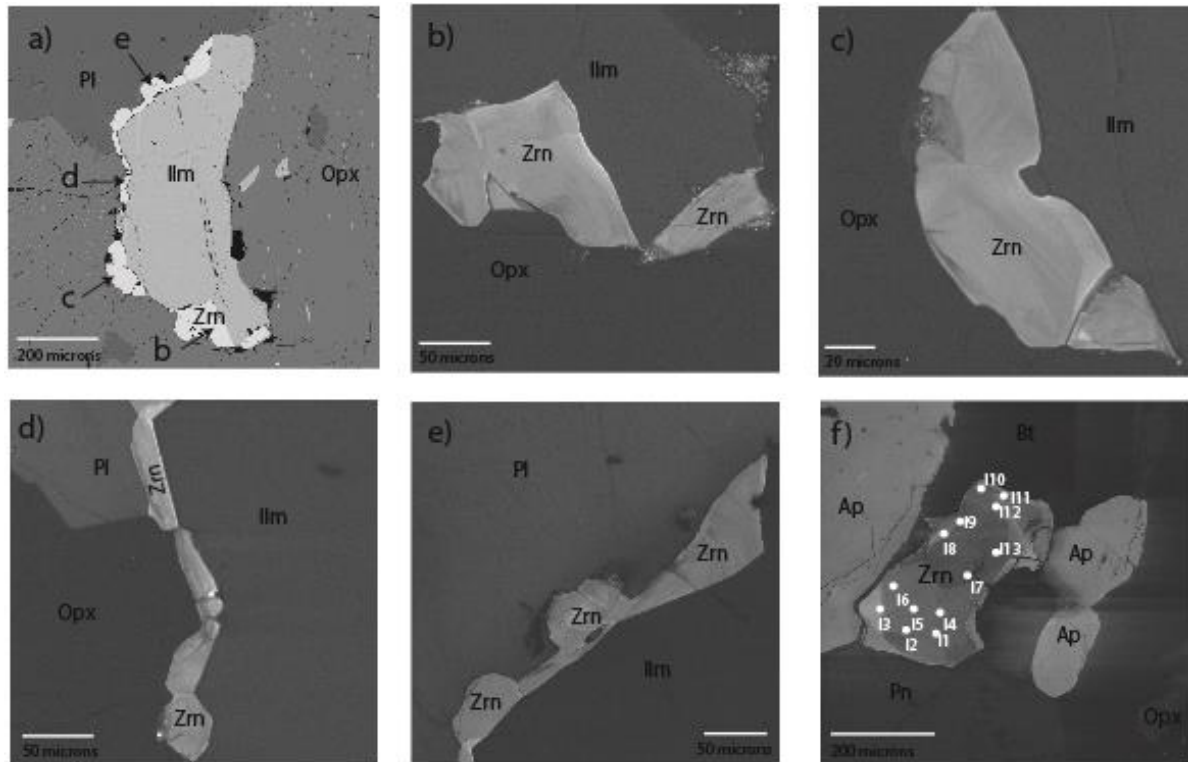


Figure 4. Cathodoluminescence (CL) (a-e) and backscattered electron (f) images of zircon grains in magmatic sample 216342. White spots represent location of analysis and corresponding spot identification numbers are noted next to spot.

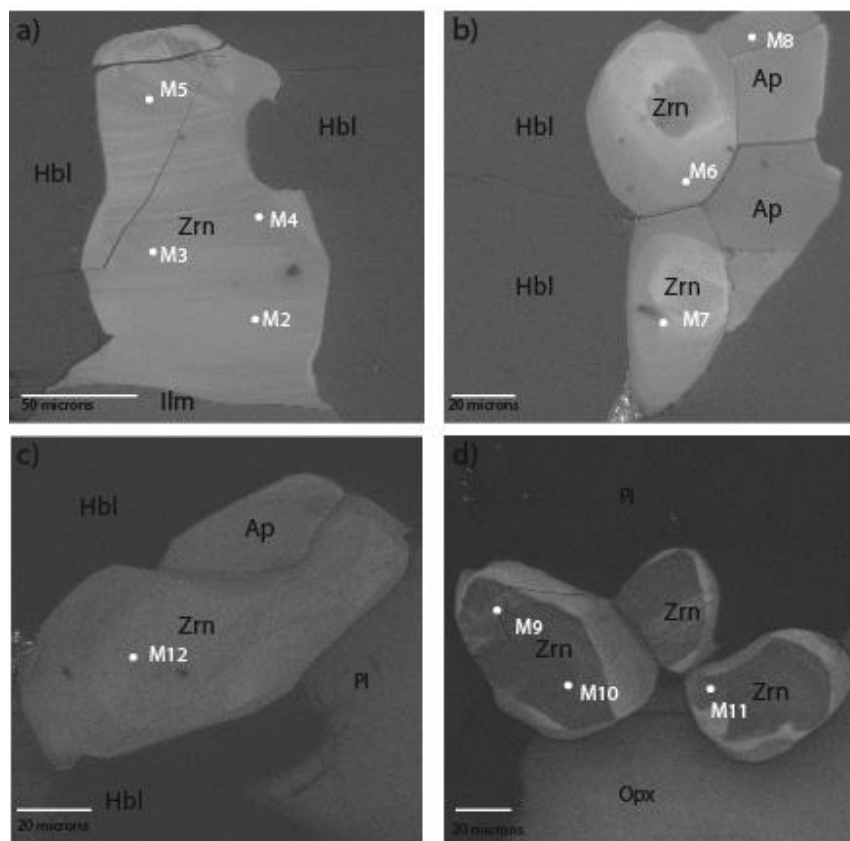


Figure 5. Cathodoluminescence (CL) (a-d) images of zircon grains in metamorphic sample 183623. White spots represent location of analysis and corresponding spot identification numbers are noted next to spot.

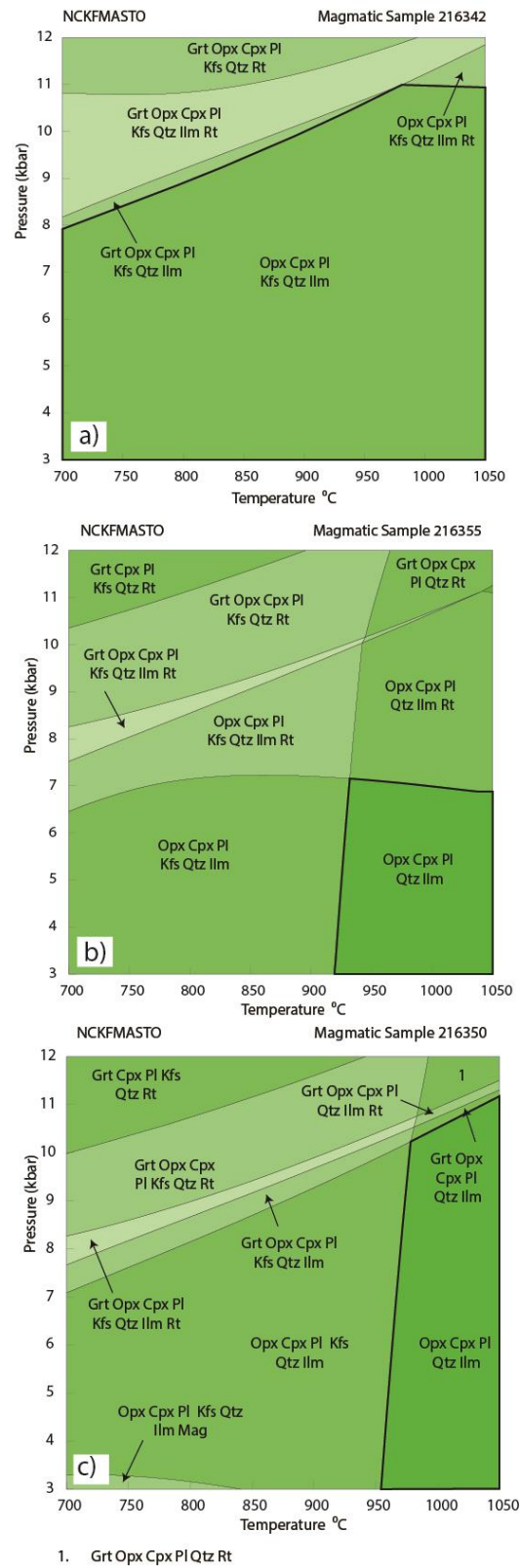


Figure 6. Calculated pseudosections for the magmatic samples a) 216342, b) 216355 and c) 216350. Solid black lines represent the crystallisation mineral assemblage for each sample (see Appendix 3 for compositional data).

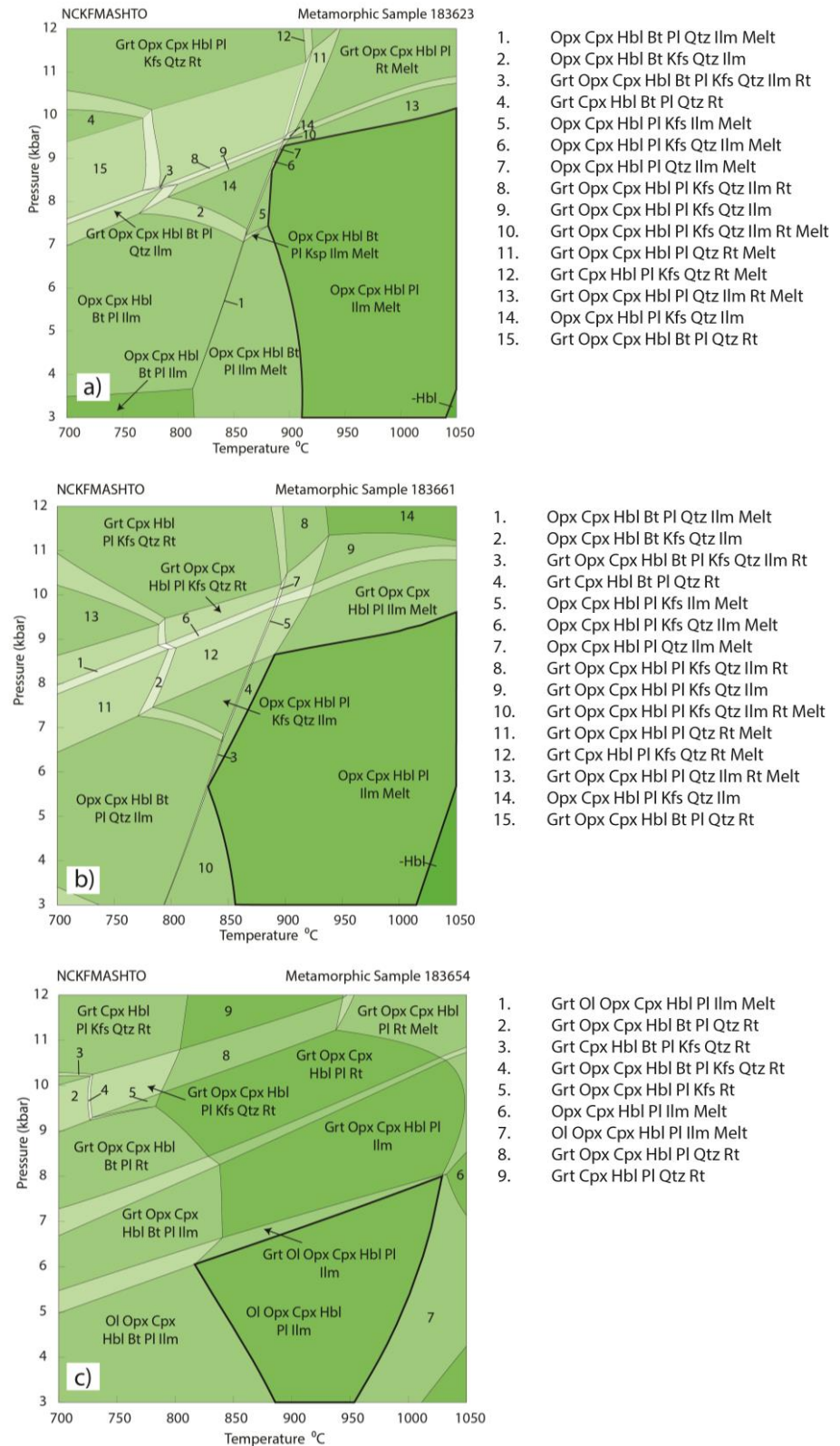


Figure 7. Calculated pseudosections for the metamorphic samples a) 183623, b) 183661 and c) 183654. Solid black lines represent the peak mineral assemblage for each sample (see Appendix 3 for compositional data).

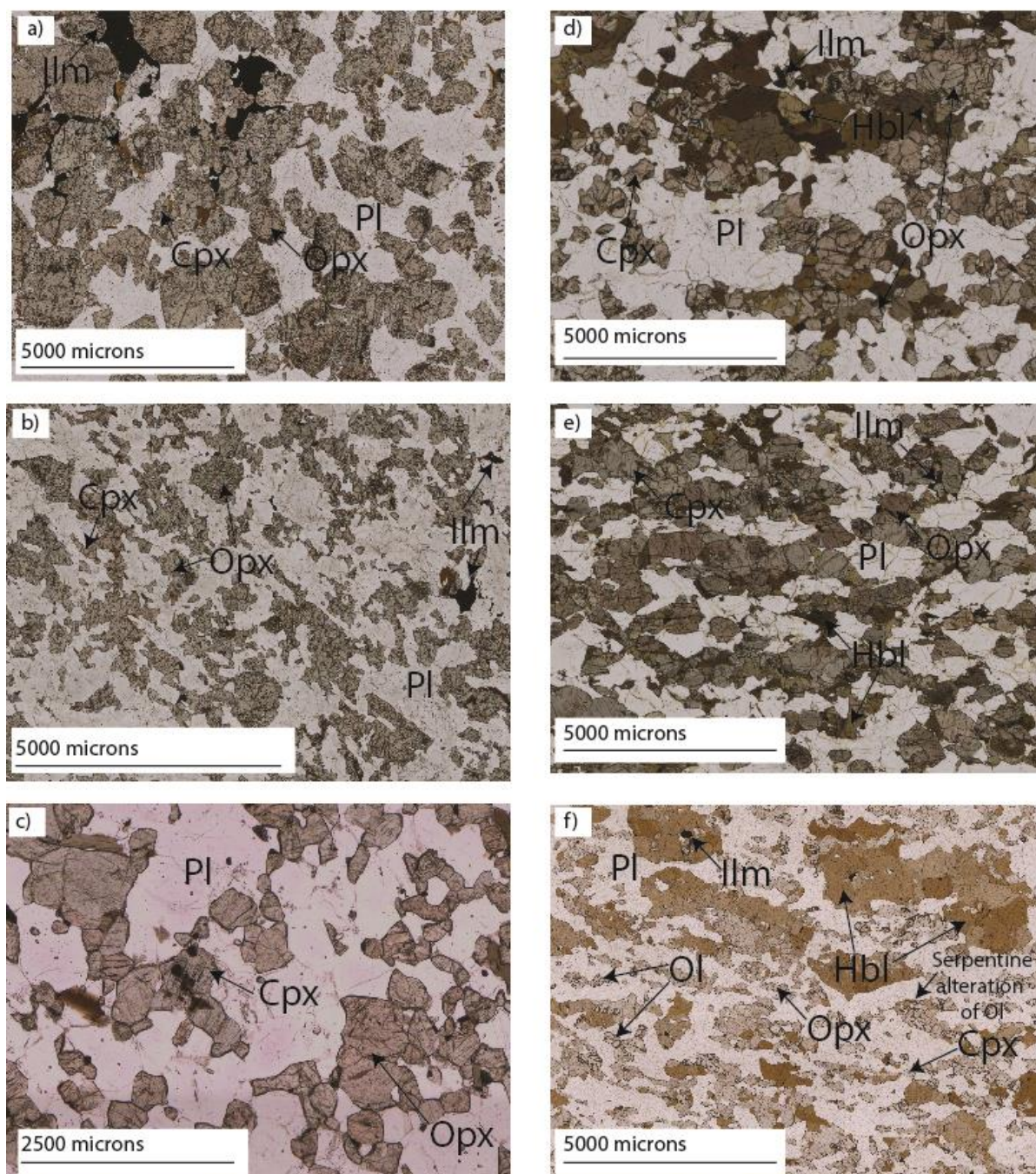


Figure 8. Photomicrographs highlighting the general textures and mineral assemblages observed. a) magmatic sample 216342, medium grained rock, orthopyroxene, clinopyroxene, plagioclase, orthoclase and ilmenite form the peak assemblage with quartz (not featured) b) magmatic sample 216355, displaying primary igneous layering textures, peak assemblage containing orthopyroxene, clinopyroxene, plagioclase, ilmenite and quartz (not featured). c) magmatic sample 216350, finer grained sample of the magmatic gabbros, contains a peak assemblage of orthopyroxene, clinopyroxene, plagioclase, quartz and ilmenite (latter two not featured here). d) Metamorphic sample 183623, peak assemblage includes orthopyroxene, clinopyroxene, hornblende, plagioclase, ilmenite and melt. e) Metamorphic sample 183661, foliation defined by the alignment of hornblende and biotite, peak assemblage of orthopyroxene, clinopyroxene, hornblende, plagioclase, ilmenite and melt. f) Metamorphic sample 183654, foliated medium grained rock. Foliation defined by prismatic hornblende, olivine crystals show evidence of serpentine alteration. Peak assemblage includes olivine, orthopyroxene, clinopyroxene, hornblende, plagioclase and ilmenite.

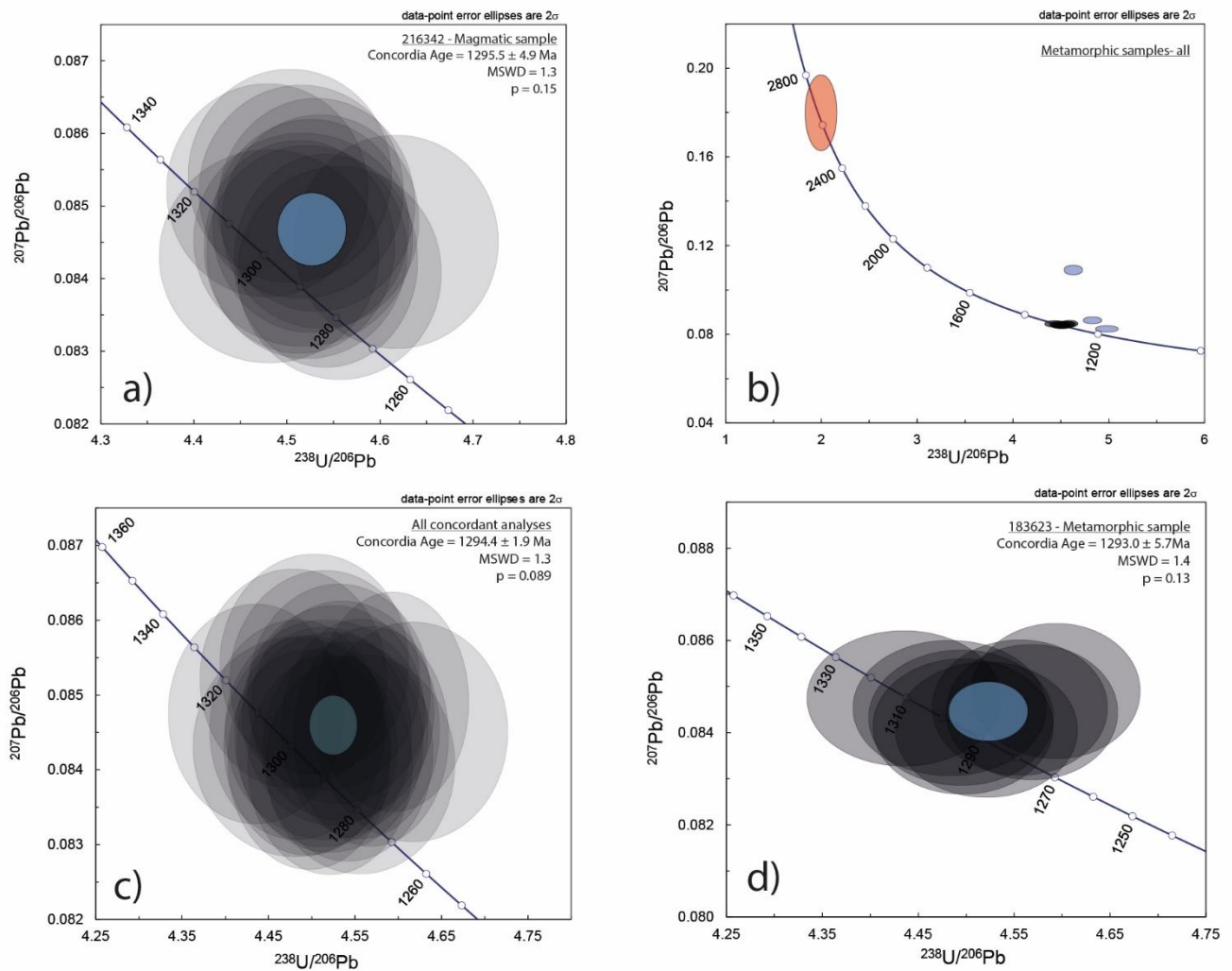


Figure 9. Tera Wasserburg concordia plot of zircon grains analysed by LA-ICP-MS in thin section. a) Zircons analysed in magmatic sample 216342. b) All data from metamorphic zircons, including discordant data. c) All concordant analyses from both magmatic and metamorphic samples. d) Concordant zircon analyses of metamorphic sample 183623. The blue ellipses represent where the all analyses overlap each other.

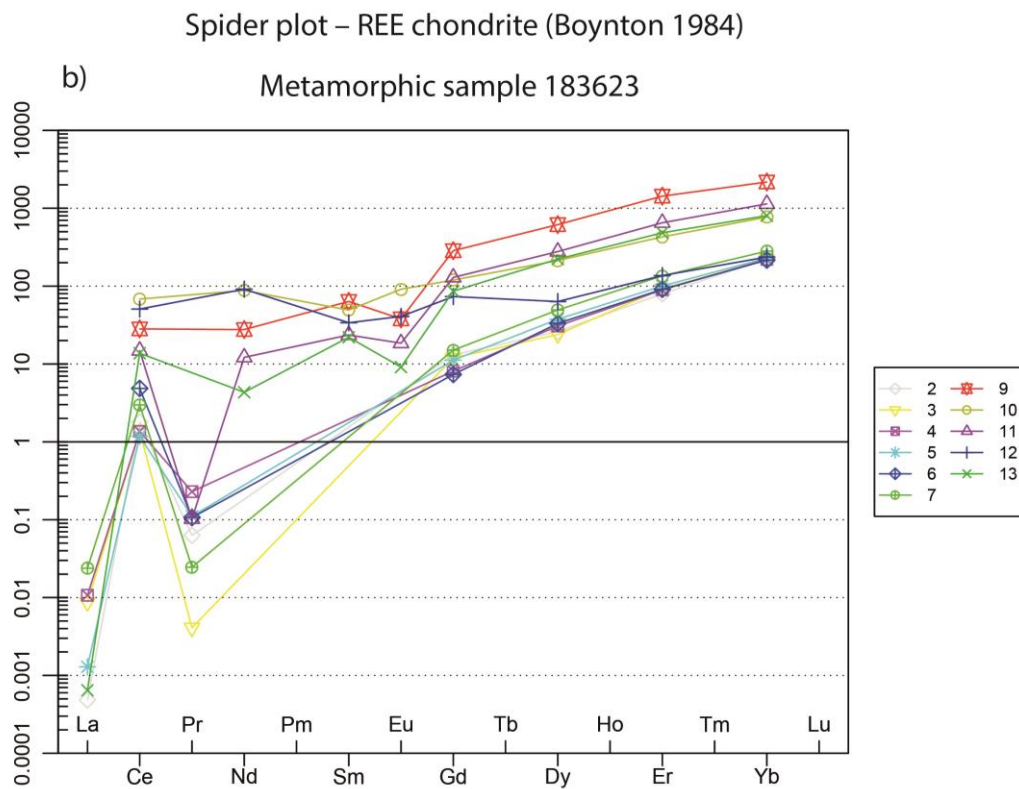
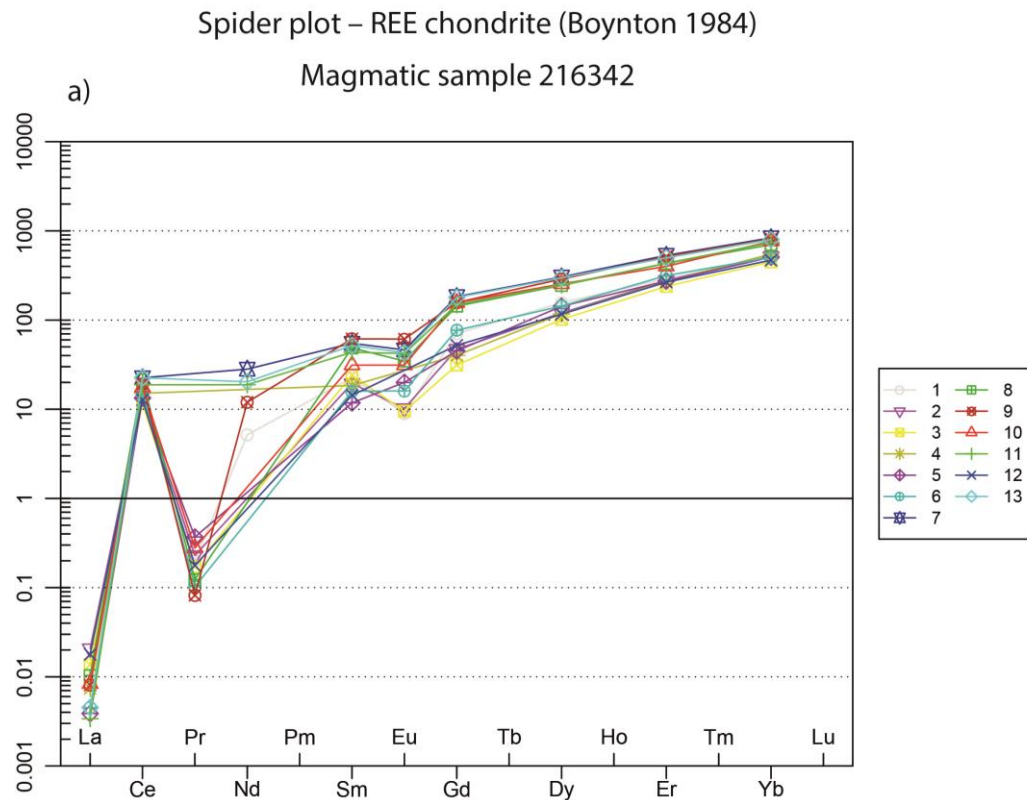


Figure 10. REE composition of zircons within magmatic gabbro (216342) (a) and from metamorphosed gabbro (183623) (b) from the Fraser Zone, WA. Normalised to CL Chondrite.

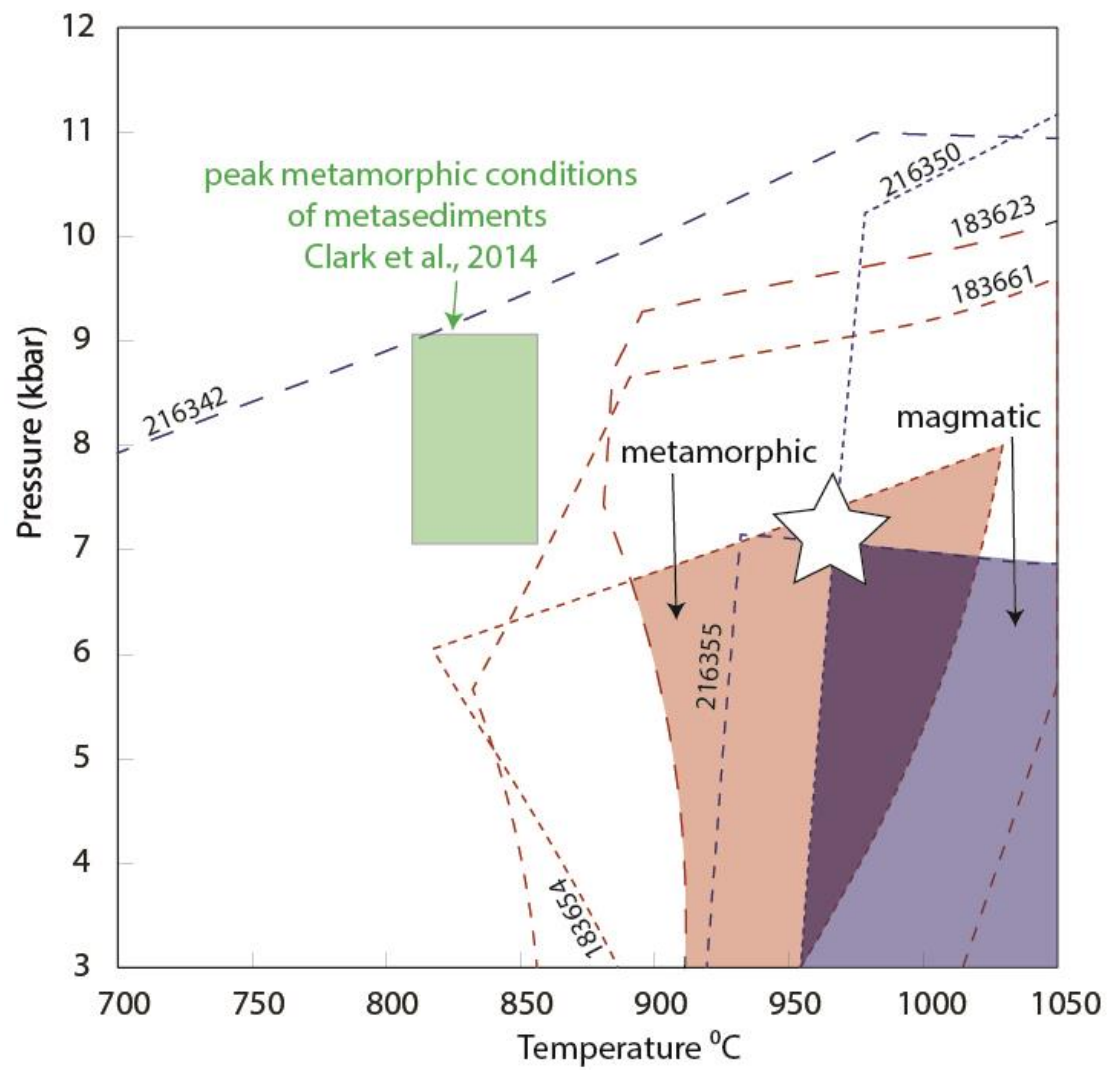


Figure 11. Compilation of pseudosections from the gabbroic rocks of the Fraser Zone, constraining the peak conditions of these rocks in the area. Green box represents the already constrained conditions of the metapelites of the Fraser Range Metamorphics from Clark et al., (2014). White star is the inferred peak crystallisation/metamorphic conditions recorded by the (meta) gabbroic rocks studied in this paper.

Tables

Primary phases / Mass % of phase [%]	Sample 216350	Sample 216355	Sample 216342
Plagioclase	50 – 55	55 – 60	30 – 35
Orthopyroxene	20 – 25	20	55 – 60
Diopside	20 – 25	15 – 20	5
Quartz	<5	2	2
Biotite	1	1	5
Ilmenite	1	<2	1
Magnetite	2	0	<1
Total	100.00	100.00	100.00

Table 1. Main mineral percentage compositions of the magmatic gabbroic samples; 216350, 216355 and 216342. These percentages are approximate and were compiled using TESCAN Integrated Mineral Analyser and optical petrology data.

Primary phases / Mass % of phase [%]	Sample 183623	Sample 183661
Plagioclase	50	45 – 50
Orthopyroxene	20 – 25	20 – 25
Hornblende	15	15 – 20
Diopside	10	15
Ilmenite	2	2
Biotite	2	-
Quartz	1 – 2	2
Hematite/Magnetite	<1	<2
Apatite	-	0.4
Total	100	100

Table 2. Main mineral percentage compositions of the metamorphic gabbroic samples; 183623 and 183661. These percentages are approximate and were compiled using TESCAN Integrated Mineral Analyser and optical petrology data.

Appendices

Appendix 1. Details of sample locations

<u>Magmatic drillcore samples:</u>								
Sample ID	Latitude	Longitude	Easting	Northing	Prospect	Diamond Core ID	Depth from (m)	Depth to (m)
216342	-32.22917	122.902844	490846	6434158	Plato	PLDT001	299.68	300.00
216350	-32.22917	122.902844	490846	6434158	Plato	PLDT001	459.05	459.36
216355	- 32.229239	122.898684	490454	6434150	Plato	PLDT003	348.41	348.66
<u>Metamorphic field samples:</u>								
Sample ID	Latitude	Longitude	Easting	Northing	Locality			
183661	-32.02916	122.81244	482290	6456317	Wyralinu Hill			
183623	-32.2451	122.76259	477635	6432372	Southwest of Mt. Malcolm			
183654	-32.23277	122.86172	486972	6433755	Mt. Malcolm			

Table 1. Detailed description of the sample locations of those utilised in this study.

Appendix 2. TESCAN Integrated Mineral Analyser (TIMA) data

Mineral compositions were attained using the TIMA and are displayed in the table below. Table 1 and 2 correspond to magmatic and metamorphosed samples respectively. Phase maps from TIMA analyses are given for magmatic and metamorphic samples in Figure 1 and 2 below respectively.

Primary phases / Mass % of phase [%]	Sample 216350	Sample 216355	Sample 216342
Plagioclase	52.35	55.63	31.35
Orthopyroxene	22.48	20.67	56.6
Diopside	15.43	17.61	3.46
Quartz	3.54	0.99	2.43
Biotite	1.18	1.08	2.24
Orthoclase	2.4	1.07	0.91
Ilmenite	0.96	1.15	0.75
Pyrrhotite	0.13	0.02	0.55
Apatite	0.13	0.18	0.24
Hematite/Magnetite	0.28	0.03	0.01
Muscovite	0.08	0.12	0.02
Pyrite	0.04	0.05	0.13
Pentlandite	0.01	0	0.16
Chalcopyrite	0.01	0.01	0.05
Rutile	0	0	0.04
Calcite	0.01	0.01	0.01
Zircon	0	0	0.02
Kaolinite	0.01	0	0
Unclassified	0.95	1.36	1.03
The rest	0	0.01	0
Total	100	100	100

Table 1. Mineral mass percentages of identified phases for the magmatic gabbroic samples. All data has been produced by the TESCAN Integrated Mineral Analyser (TIMA).

Primary phases / Mass % of phase [%]	Sample 183623	Sample 183661
Plagioclase	49.12	44.28
Orthopyroxene	24.5	22.86
Hornblende	14.29	15.68
Diopside	8.67	12.42
Ilmenite	0.31	1.37
Biotite	1.31	0.16
Quartz	0.35	0.91
Apatite	0.37	0.4
Orthoclase	0.24	0.4
Hematite/Magnetite	0.3	0.28
Calcite	0	0.04
Pyrrhotite	0.03	0
Muscovite	0.01	0.02
Garnet	0	0.02
Zircon	0.01	0
Osumilite	0.01	0
Unclassified	0.48	1.15
The rest	0	0.01
Total	100	100

Table 2. Mineral mass percentages of identified phases for the metamorphosed gabbroic samples. All data has been produced by the TESCAN Integrated Mineral Analyser (TIMA).

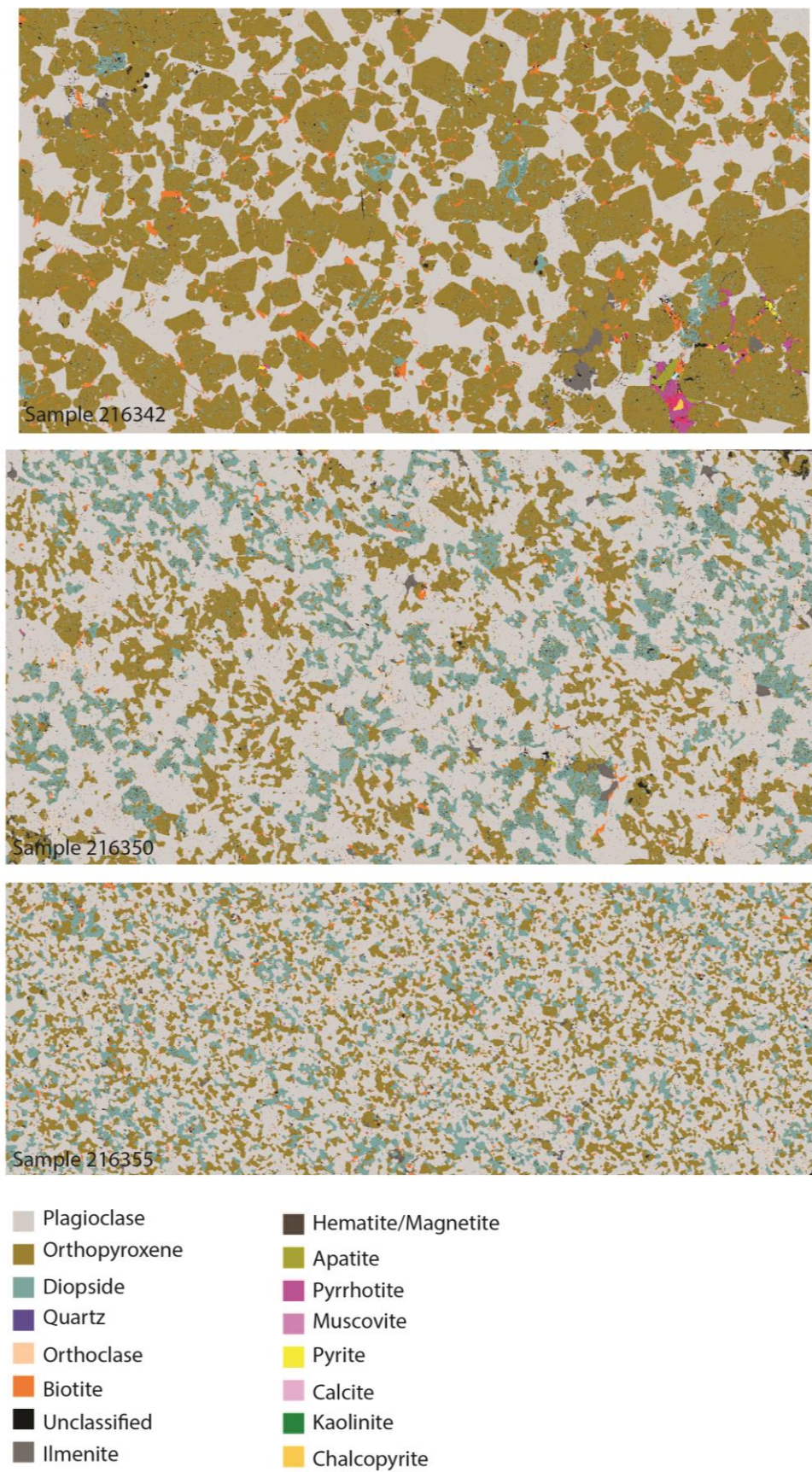


Figure 1. TIMA phase maps of magmatic samples.

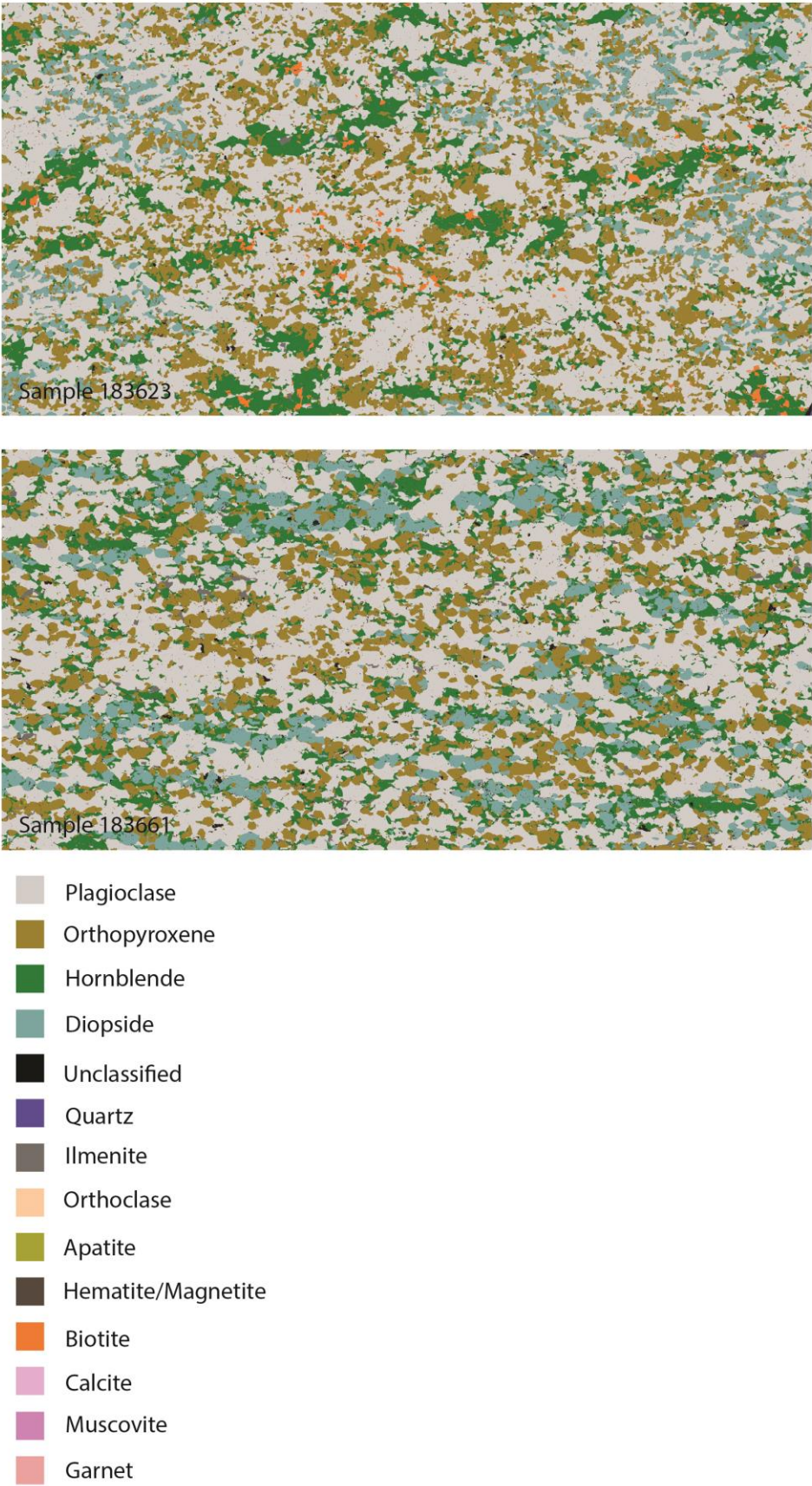


Figure 2. TIMA phase maps of metamorphic samples.

Appendix 3. XRF bulk composition analysis

XRF bulk composition analysis for each sample are displayed in the corresponding tables below.

	Mol% with Fe³/ Σ Fe=0.2		
Sample number	216350	216342	216355
SiO₂	54.07	50.83	55.5
TiO₂	0.53	0.48	0.52
Al₂O₃	10.28	5.26	10.14
FeO	8.18	10.68	6.56
MgO	12.88	25.95	13.51
CaO	11.28	5.57	11.26
K₂O	0.31	0.18	0.25
Na₂O	2.43	1.02	2.23
H₂O	0	0	0
Total	100	100	100
O	0.41	0.53	0.33
10%	0.82	1.07	0.66

Table 3. XRF analysis data showing the major oxide composition (weight% for all magmatic samples modelled).

	Mol% with Fe³/ Σ Fe=0.2		
Sample number	183654	183661	183623
SiO₂	47.15	50.13	50.77
TiO₂	0.81	1.06	0.84
Al₂O₃	10.58	10.19	10.49
FeO	8.65	10.28	8.54
MgO	14.67	12.89	13.99
CaO	10.81	10.53	10.86
K₂O	0.15	0.36	0.39
Na₂O	2.14	2.30	2.33
H₂O	5.01	2.18	1.71
Total	100.00	100.00	100.00
O	0.43	0.51	0.43
10%	0.86	1.03	0.85

Table 4. XRF analysis data showing the major oxide composition (weight% for all metamorphic samples modelled).

Appendix 4. Petrographic descriptions

Sample 216355

Mineral notes

1. Clinopyroxene (CPX) ~ 30%

- Most commonly subhedral pale green grains, average diameter of 0.9 mm
- Interleaved with orthopyroxene, forming around the edges of subhedral plagioclase grains
- May form exsolution lamellae in the orthopyroxene grains
- Rounded opaque minerals are interstitial, occur along the CPX/OPX grain boundaries and as inclusions

2. Orthopyroxene (OPX) ~16%

- Morphologically similar to clinopyroxene, average diameter of 1.5 mm
- Shows distinct pleochroism pale pink to pale green
- Less abundant than CPX
- May contain exsolution lamellae of CPX
- Exsolution lamellae appears brown in PPL, in XPL often shows high birefringence second order blue – exsolution of clinopyroxene
- Contain exsolution of aligned elongate biotite grains (on average 120 μm)

3. Biotite ~5%

- Elongate, brown euhedral to subhedral grains
- Small grains on average 0.2-0.5mm
- Appear as exsolution within pyroxene grains? Aligned along cleavage planes?
- Appear as inclusions within pyroxene grains, often found around elongate opaque minerals (ilmenite?)
- Generally, found along grain boundaries of pyroxenes and occasionally as inclusions

4. Plagioclase ~43%

- Subhedral laths on average 1.5mm in grain size
- In some cases, plagioclase laths are found enclosed within pyroxene grains – plagioclase crystallised first?

5. Quartz 3%

- Anhedral grains, show undulose extinction

- Maximum grain size 1.5mm

6. Opaques 4%

- Two distinct opaques. The first forms anhedral blobs (average 0.2mm) that are interstitial and form along grain boundaries of mostly pyroxene grains – magnetite?
- The second is commonly associated with biotite grains and is subhedral to elongate, a maximum grain size of 0.5mm. – ilmenite

Sample 216342

Mineral notes

1. Orthopyroxene

- Generally larger than CPX
- Comprise ~ 30 vol.% of the sample
- Subhedral grains with an average diameter of ~ 2 mm
- Distinct uneven fractures
- Distinct exsolution – precipitation of ilmenite platelets

2. Clinopyroxene

- Lower relief than OPX
- Comprise ~ 20 vol.% of sample
- Average diameter of ~ 1 mm
- Similarly, to OPX distinct form of exsolution of ilmenite lamellae platelets
- Contains uneven fractures (less than in OPX) – they contain alteration dark brown colour in PPL

3. Plagioclase

- On average ~ 2mm in size
- Comprise ~ 30 vol.% of sample
- Anhedral to subhedral grains and show sericitic alteration
- Distinct lamellae twinning

4. Biotite

- Comprise ~ 15 vol.% of the sample
- Generally, found along grain boundaries of both OPX and CPX as elongate, euhedral to subhedral

- Found as inclusions in both pyroxenes
- Randomly oriented throughout the section

5. Opaques

- Two distinct types; ~5 vol.%
- The first – much larger (average ~ 4 mm) – fills the gaps between closely spaced pyroxene grains
- The second -smaller (average ~ 0.4 mm) – forms as inclusions within pyroxenes/ biotite and along grain boundaries of these minerals too – possibly magnetite?

6. Sulphides

- Can see a silvery/gold, elongate mineral with naked eye on thin section
- Under thin section it seems to fill free gap space between pyroxene grains and is opaque, approx. ~1vol.%

7. Zircon

- Discontinuous corona surrounding ilmenite
- Very small zircons on average ~ 25 microns
- Dusty appearance in PPL and third order birefringence colours in XPL

Sample 216350

Mineral notes

1. Clinopyroxene

- Comprise ~ 20% of sample
- Anhedral to sub rounded grains on average ~ 1 mm in size
- Contains oriented exsolution of ilmenite platelets

2. Orthopyroxene

- Anhedral sub rounded grains ~ 15%
- Average grain size 1mm
- Oriented exsolution
- Pleochroism: pale pink to pale green

3. Plagioclase

- Comprise ~50% of the sample
- Average size 1 mm
- Sericitic alteration

- Subhedral laths with distinct lamellae twinning
4. Biotite
 - Subhedral, elongate grains average size of 0.4 mm
 - As inclusions within pyroxene grains
 - Comprise ~ 5 vol.% of the sample
 5. Quartz
 - Undulose extinction
 - ~ < 5 vol.% of the sample
 6. Opaques
 - Smaller blobs of opaques form on grain boundaries of pyroxenes and biotite – likely to be magnetite average size are ~200 microns
 - ~ < 2 vol.% of the sample
 - Some larger opaques that seem to fill the gaps between pyroxene and plagioclase – possible sulphides (average size ~ 1mm in size)

Sample 183623

Mineral notes

1. Clinopyroxene
 - Comprise ~15% of sample
 - Anhedral to sub rounded grains on average ~ 1 mm in size
2. Orthopyroxene
 - Anhedral to subhedral grains, 20 vol.% of sample
 - Average grain size 1mm
 - Contains inclusions of hornblende and plagioclase
 - OPX and CPX are interleaved together
3. Plagioclase
 - Comprise ~30% of the sample
 - Average size 1 mm
 - Subhedral laths
 - Complex zoning
4. Hornblende
 - 15 vol.% of the sample

- Brown, subhedral elongate to prismatic shape
 - Shows exsolution similar to that in the magmatic samples
 - Opaque blobs around grain boundaries (magnetite?)
5. Biotite
- Subhedral, elongate grains average size of 0.5 mm
 - Occurs on the grain boundaries of mainly hornblende
 - Comprise ~ 5 vol.% of the sample
6. Quartz
- Undulose extinction
 - On average 0.5 mm in length
 - ~ < 5 to ~ 10 vol.% of the sample
7. Opaques
- Potentially ilmenite – occurs with biotite and forms elongate grains
 - Magnetite? – small rounded blobs occur close to biotite grains
 - ~ 10 vol.% of the sample
8. Accessory minerals
- Potentially high relief (apatite) sub rounded – forms in clusters along grain boundaries of hornblende
 - Possible zircon – high relief prismatic shape

Sample 183654

Mineral notes

1. Clinopyroxene
 - ~ 15 % of the sample
2. Orthopyroxene
 - ~ 20% of the sample, subhedral to elongate (very similar morphologically to clinopyroxene)
 - Pink to pale green pleochroism
 - Contains inclusions of hornblende and plagioclase
 - Grain size on average ~ 1 mm
 - Contains olivine inclusions?
3. Hornblende

- Subhedral , prismatic grains that are on average ~ 1mm in length
- ~ 20% of the sample

4. Olivine

- Comprise ~ 10 vol.%
- High relief- uneven fractures
- On average 0.3 mm
- Hydrated – observed by the green alteration (serpentine) mainly along the fractures and outer grain boundaries

5. Plagioclase

- Anhedral to subhedral laths, ~ 28 vol.% of the sample
- Twinning – lamellae

6. Biotite

- Elongate subhedral grain on average ~ 0.5 mm
- ~ 2 vol.% of the sample

7. Opaques

- ~ 5 vol.% of the sample
- Anhedral blobs which cluster around grain boundaries-possibly magnetite

Sample 183661

Mineral notes

1. Clinopyroxene

- ~ 20 % of the sample, subhedral to elongate grains which are sub parallel to the foliation
- Distinct pale green in colour (weakly pleochroic to a lighter shade of green)
- Appears to have iron staining? (yellow alteration evident over most of the sample) and concentrates along fractures
- Contains inclusions of opaque minerals
- Associated with orthopyroxene and hornblende

2. Orthopyroxene

- ~ 25% of the sample, subhedral to elongate (very similar morphologically to clinopyroxene)
- Pink to pale green pleochroism

- Exsolution – dark brown oriented
- On average grains are ~ 1 mm in length

3. Hornblende

- Elongate, subhedral grains that are on average ~ 1mm in length
- ~ 15% of the sample
- Show exsolution
- Grain boundaries often contain small opaque minerals clustered
- Mainly forms along the rims/ boundaries of subhedral pyroxene grains

4. Plagioclase

- Subhedral laths, ~ 30 to 35% of the sample
- Commonly show sericitic alteration
- Twinning – lamellae
- Contains inclusions of accessory phases – apatite?

5. Quartz

- Granoblastic
- Undulose extinction
- Anhedral grains (~ 0.5 to ~ 1 mm)

Appendix 5. U–Pb geochronology data

Group	Spot	Grain.	^{238}U	^{232}Th	^{232}Th	206Pb/204Pb	$^{238}\text{U}/^{206}\text{Pb}^*$		$^{207}\text{Pb}^*/^{206}\text{Pb}^*$		$^{238}\text{U}/^{206}\text{Pb}^*$		$^{207}\text{Pb}^*/^{206}\text{Pb}^*$		Disc.
ID	no.	spot	(ppm)	(ppm)	^{238}U		$\pm 2s$		$\pm 2s$		date (Ma) $\pm 2s$		date (Ma) $\pm 2s$		(%)
216342	1	d	180.2	181.7	0.984	48000	4.5025	0.0892	0.0854	0.0012	1293	23	1324	27	2.36
216342	2	d	173.2	115.3	1.49	72000	4.5147	0.0897	0.0852	0.0012	1290	23	1319	28	2.20
216342	3	d	158.6	107.7	1.4654	70000	4.5351	0.0864	0.0848	0.0012	1285	22	1310	28	1.89
216342	4	d	180.1	122.5	1.471	128000	4.4783	0.0882	0.0852	0.0012	1299	23	1320	27	1.56
216342	5	d	184.6	122.4	1.5022	130000	4.4803	0.0964	0.0843	0.0012	1299	25	1299	27	-0.02
216342	6	d	181.7	204.5	0.8841	107000	4.5126	0.0835	0.0844	0.0012	1290	22	1302	27	0.91
216342	7	d	297	356	0.8296	120000	4.5249	0.0860	0.0847	0.0012	1287	22	1308	27	1.64
216342	8	d	289.2	343	0.8392	218000	4.5413	0.0804	0.0843	0.0012	1283	21	1297	27	1.11
216342	9	d	265.9	351	0.7537	162000	4.5208	0.0879	0.0844	0.0012	1288	23	1300	27	0.92
216342	10	d	178.6	263.1	0.6762	116000	4.5558	0.0892	0.0841	0.0012	1279	23	1294	27	1.13
216342	11	d	219.1	285.1	0.7629	187000	4.6168	0.0895	0.0845	0.0012	1264	22	1303	27	3.02
216342	12	d	156.1	177.8	0.8751	131000	4.5167	0.0959	0.0845	0.0012	1289	25	1304	27	1.15
216342	13	d	269	351	0.7631	200000	4.5310	0.0862	0.0850	0.0012	1286	22	1315	26	2.21
183623	2	a	213.6	134.1	1.5893	60000	4.5935	0.0717	0.0849	0.0012	1270	18	1313	27	3.25
183623	3	a	235	157	1.4949	-2000000	4.5558	0.0747	0.0846	0.0012	1279	19	1304	27	1.94
183623	4	a	243	175.4	1.3809	-320000	4.5683	0.0730	0.0845	0.0012	1276	18	1302	27	2.01
183623	5	a	215.6	145.7	1.4772	600000	4.5208	0.0777	0.0841	0.0012	1288	20	1293	27	0.41
183623	6	b	187.8	147.5	1.271	100000	4.4944	0.0788	0.0843	0.0012	1295	21	1301	25	0.46
183623	7	b	126.9	85.6	1.4825	350000	4.8333	0.0794	0.0864	0.0013	1212	18	1346	28	9.93
183623	8	b	143.9	97.4	1.479	1000000	4.4346	0.0826	0.0848	0.0012	1311	22	1309	27	-0.16
183623	9	d	6.2	5.3	1.14	30200	1.9960	0.1355	0.1800	0.0140	2610	140	2660	130	1.88
183623	10	d	613	873	0.6998	1500000	4.4964	0.0768	0.0841	0.0012	1294	20	1295	27	0.07
183623	11	d	582	1505	0.3863	80000000	4.9826	0.0968	0.0825	0.0012	1179	21	1256	28	6.16
183623	12	c	338.8	376.4	0.8985	1060000	4.4823	0.0824	0.0845	0.0012	1298	22	1304	28	0.47

Table 5. Summary of LA-ICPMS U–Pb zircons results for all samples.

Appendix 6. Trace element geochemistry data

Spot number	La	Ce	Pr	Nd	Sm	Eu	Gd	Dy	Er	Yb
1	0.0029	12.3	0.02454	3.1	4.4	0.66	18.3	50.3	61.2	107.8
2	0.00644	11.5	0.028	Below LOD	3.8	0.75	12.2	38.7	58.3	108.5
3	0.00423	9.4	0.021	Below LOD	4.7	0.7	8.1	32.8	50	93.8
4	0.0023	12.2	0	Below LOD	3.6	Below LOD	10.4	37.8	57	115
5	-0.0024	10.8	0.045	Below LOD	2.3	1.47	11.7	45.9	57.6	105.9
6	0.0014	12.23	-0.025	Below LOD	3.1	1.18	19.9	46.2	66.2	105.6
7	Below LOD	18.2	Below LOD	16.9	10.7	3.4	47.4	97.9	111.6	174.7
8	0.0032	17.3	-0.03	Below LOD	9.5	2.55	37.1	78.7	90.7	146.3
9	0.0025	15.5	-0.02	7.2	12	4.5	40.7	92.8	108.5	169.4
10	0.0026	14.2	0.03386	Below LOD	6.1	2.3	40.6	81.9	84	160
11	-0.0021	15.2	Below LOD	11.3	8.5	3.1	38.5	79.8	91.1	154.8
12	0.00553	10.3	0.02159	Below LOD	2.8	Below LOD	13.5	37.5	55.8	98.1
13	0.0014	18.2	Below LOD	12.2	10.1	3.16	46.4	96	104.7	167

Table 6. Trace element amounts (ppm) in zircon from magmatic sample 216342 with corresponding spot numbers. Refer to BSE and CL images in Fig. 4 for exact locations of spot numbers. Below LOD stands for below limit of detection.

Spot number	La	Ce	Pr	Nd	Sm	Eu	Gd	Dy	Er	Yb
2	-0.0003	1.45	0.00768	Below LOD	Below LOD	Below LOD	3.4	8.4	16.7	46.7
3	0.0027	1.11	-0.001	Below LOD	Below LOD	Below LOD	3.1	7.7	19.4	45.9
4	0.00332	1.1	0.028	Below LOD	Below LOD	Below LOD	2.1	9.9	18.8	46.1
5	0.0004	0.95	-0.027	Below LOD	Below LOD	Below LOD	2.9	12.1	21.1	47.9
6	Below LOD	3.92	-0.026	Below LOD	Below LOD	Below LOD	1.9	10.7	19.1	45.1
7	0.00739	2.41	0.003	Below LOD	Below LOD	Below LOD	3.9	15.9	28.4	58.8
9	Below LOD	22.8	Below LOD	16.6	12.4	2.79	73.8	198.4	300.5	454
10	Below LOD	55.2	Below LOD	52.8	9.6	6.7	31	68.6	90.1	161
11	Below LOD	12	-0.025	7.3	4.6	1.36	33.5	89.5	136.7	237.9
12	Below LOD	41	Below LOD	54.8	6.6	3	19	20.4	28.7	49.4
13	0.0002	11.1	Below LOD	2.6	4.3	0.67	22.3	71.6	101.7	168

Table 7. Trace element amounts (ppm) in zircons from magmatic sample 183623 with corresponding spot numbers. Refer to BSE and CL images in Fig. 5 for exact locations of spot numbers.

A PETROGRAPHIC AND GEOCHRONOLOGICAL ASSESSMENT OF
THE GABBROIC AND METAGABBROIC ROCKS OF THE FRASER
ZONE, ALBANY-FRASER OROGEN, WESTERN AUSTRALIA

This Record is published in digital format (PDF) and is available as a free download from the DMIRS website at
<www.dmp.wa.gov.au/GSWApublications>.

Further details of geological products produced by the Geological Survey of Western Australia can be obtained by contacting:

Information Centre
Department of Mines, Industry Regulation and Safety
100 Plain Street
EAST PERTH WESTERN AUSTRALIA 6004
Phone: +61 8 9222 3459 Fax: +61 8 9222 3444
www.dmp.wa.gov.au/GSWApublications

